

# Optimal a priori estimates for higher order finite elements for elliptic interface problems

Jingzhi Li<sup>a,1</sup>, Jens Markus Melenk<sup>b</sup>, Barbara Wohlmuth<sup>c,\*</sup>, Jun Zou<sup>a,2</sup>

<sup>a</sup> Department of Mathematics, The Chinese University of Hong Kong, Shatin, N.T., Hong Kong

<sup>b</sup> Institut für Analysis und Scientific Computing, Technische Universität Wien, Austria

<sup>c</sup> Institut für Angewandte Analysis und Numerische Simulation (IANS), Universität Stuttgart, 70569 Stuttgart, Germany

## ARTICLE INFO

### Article history:

Received 10 June 2008

Received in revised form 22 July 2009

Accepted 4 August 2009

Available online 25 August 2009

MSC:

65N12

65N30

### Keywords:

Elliptic interface problems

Higher order finite elements

Optimal convergence rates

A priori estimates

## ABSTRACT

We analyze higher order finite elements applied to second order elliptic interface problems. Our a priori error estimates in the  $L^2$ - and  $H^1$ -norm are expressed in terms of the approximation order  $p$  and a parameter  $\delta$  that quantifies how well the interface is resolved by the finite element mesh. The optimal  $p$ -th order convergence in the  $H^1(\Omega)$ -norm is only achieved under stringent assumptions on  $\delta$ , namely,  $\delta = O(h^{2p})$ . Under weaker conditions on  $\delta$ , optimal a priori estimates can be established in the  $L^2$ - and in the  $H^1(\Omega_\delta)$ -norm, where  $\Omega_\delta$  is a subdomain that excludes a tubular neighborhood of the interface of width  $O(\delta)$ . In particular, if the interface is approximated by an interpolation spline of order  $p$  and if full regularity is assumed, then optimal convergence orders  $p+1$  and  $p$  for the approximation in the  $L^2(\Omega)$ - and the  $H^1(\Omega_\delta)$ -norm can be expected but not order  $p$  for the approximation in the  $H^1(\Omega)$ -norm. Numerical examples in 2D and 3D illustrate and confirm our theoretical results.

© 2009 IMACS. Published by Elsevier B.V. All rights reserved.

## 1. Introduction

Elliptic interface problems are frequently encountered in scientific computing and industrial applications [18]. A typical example is provided by the modeling of physical processes which involve two or more materials with different properties, such as the conductivity of steel and bronze in heat diffusion. It is well known that the solutions of elliptic interface problems may have higher regularity in each individual material region than in the entire physical domain.

Numerous numerical methods for elliptic interface problems with arbitrary but smooth interfaces have been extensively studied during the last two decades; we refer to [2–4,6–8,15,16,19–21], the recent monograph [18], and the references therein for an overview. Roughly speaking, these methods can be categorized into three classes, namely, *conforming*, *non-conforming* and *IIM-related*. For conforming methods, mostly linear finite element approximations have been studied with the interface being approximated by a linear interpolating spline (see [2–4,8,21]); isoparametric elements have also been analyzed in [3]. Nonconforming methods include mortar elements [16], Nitsche techniques [15], which are closely related to DG-type methods, and interior penalty Lagrange multiplier methods [6]. In view of the efficiency of the immersed inter-

\* Corresponding author.

E-mail addresses: jzli@math.cuhk.edu.hk (J. Li), melenk@tuwien.ac.at (J.M. Melenk), wohlmuth@ians.uni-stuttgart.de (B. Wohlmuth), zou@math.cuhk.edu.hk (J. Zou).

<sup>1</sup> The work of this author was in part supported by the German Research Foundation (SPP 1146).

<sup>2</sup> The work of this author was substantially supported by Hong Kong RGC grants (Projects 404606 and 404407).

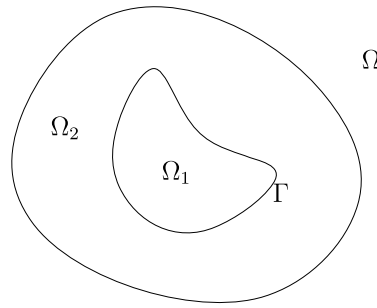


Fig. 1. Domain  $\Omega$  and its subdomains  $\Omega_1$  and  $\Omega_2$ .

face methods for rectangular domains, immersed FEMs of linear and quadratic classes in 1D and 2D on Cartesian grids are constructed and analyzed in [7,19,20].

The current work is concerned with the analysis of conforming higher order FEMs for two- and three-dimensional interface problems with smooth interfaces. If the interface is resolved exactly (e.g., using blending element techniques in [11–13]), then optimal rates of convergence can be expected in appropriate Galerkin settings. But quite often, the interface is only approximated. In this case, the mismatch between the FEM mesh and the interface raises several questions:

1. How does the approximation of the interface affect the approximation properties of FEM spaces?
2. How does the variational crime resulting from replacing the exact bilinear form with a mesh dependent one influence the a priori estimates?
3. Is the error introduced by approximating the interface localized?

The purpose of this present work is to provide answers to the above three questions. Theorems 4.1, 4.6 and the discussion in Section 4.4 address the first two questions and provide convergence results for finite elements of order  $p$  depending on the accuracy of the interface approximation. In the special case that we approximate the interface by an interpolating spline of degree  $m$ , we obtain (under appropriate regularity assumptions) a discretization error of order  $O(h^{\min\{p, (m+1)/2\}})$  in the  $H^1(\Omega)$ -norm and of order  $O(h^{\min\{p, m\}+1})$  in the  $L^2(\Omega)$ -norm. In particular, we observe optimal convergence rates both in the  $H^1(\Omega)$ - and in the  $L^2(\Omega)$ -norm for piecewise linear elements ( $p = 1$ ) and piecewise linear interpolation of the interface ( $m = 1$ ). We emphasize that for  $p > 1$  the condition on the interface approximation is more stringent for optimal convergence rates in the  $H^1(\Omega)$ -norm than in the  $L^2(\Omega)$ -norm. The condition on the interface approximation can be considerably weakened by using a different error measure. Indeed, we address the aforementioned third question in Section 4.3 by studying the  $H^1(\Omega_\delta)$ -convergence, where  $\Omega_\delta := \Omega \setminus S_\delta$  and  $S_\delta$  is a tubular neighborhood of the interface of width  $2\delta$ . We show in Theorem 4.8 that the optimal rate of convergence can be achieved in the  $H^1(\Omega_\delta)$ -norm under significantly weaker conditions on the mismatch between the interface. Returning to the 2D example of an interpolating spline of degree  $m$  discussed above, we expect  $\delta = O(h^{m+1})$  and the FEM error is then  $O(h^{\min\{p, m\}})$  when measured in the  $H^1(\Omega_\delta)$ -norm.

The present work is closely related to the earlier articles [3,4,8]. The work [3] analyzes the case of *isoparametric* elements and obtains optimal convergence rates under extra regularity assumptions (see [3, Theorem 2.1]). References [4,8] restrict their attention to the 2D case. In all three references, the interface is approximated by an interpolating spline (possibly of higher order); in contrast, the present paper does not make this assumption and merely requires the approximation to the interface to be sufficiently accurate in an appropriate sense (see Definition 3.1).

Although the detailed approximation theory is developed in this work only for a scalar elliptic model problem, analogous results can be derived for some vectorial systems such as the Lamé equations. To illustrate the applicability of our results to a more general setting, we present a linear elasticity problem in Section 5.

The rest of the paper is organized as follows. In Section 2, we introduce the problem setting and an abstract framework for approximating the interface. Using this framework, the classical affine elements, curved elements [9,27] and blending elements can be treated in a unified manner. Section 3 analyzes the approximation properties of piecewise smooth functions by conforming FEM spaces. The basic technical tools are a  $\delta$ -strip argument and a modified quasi-interpolation operator. The abstract approximation results of Section 3 are applied to the FEM in Section 4 and optimal a priori estimates are obtained in different norms. Several numerical examples illustrate in Section 5 our theoretical results.

## 2. Elliptic interface problem

In this work, we will develop a general convergence theory for conforming finite element methods for elliptic interface problems. Let  $\Omega$  be a bounded Lipschitz domain in  $\mathbb{R}^d$ ,  $d = 2, 3$  which is assumed to consist of two Lipschitz subdomains  $\Omega_1$ ,  $\Omega_2$  with  $\Omega_1 \subset \subset \Omega$ ,  $\Omega_2 := \Omega \setminus \overline{\Omega_1}$ , and the interface  $\Gamma := \partial\Omega_1$  (see Fig. 1) is required to have at least  $C^2$ -regularity.

For simplicity of notation, we will restrict ourselves to the following elliptic interface problem:

$$-\nabla \cdot (\beta \nabla u) = f \quad \text{in } \Omega, \quad u = 0 \quad \text{on } \partial\Omega; \quad (1)$$

the jump conditions on the interface for the solution and the flux are given by:

$$[u] = 0 \quad \text{on } \Gamma, \quad \left[ \beta \frac{\partial u}{\partial n} \right] = 0 \quad \text{on } \Gamma, \quad (2)$$

where  $[u] := u_1|_{\Gamma} - u_2|_{\Gamma}$  and  $[\beta \partial u / \partial n] := \beta_1 \partial u_1 / \partial n_1 + \beta_2 \partial u_2 / \partial n_2$ . Here  $u_i$  stands for the restriction of  $u$  to  $\Omega_i$ , and  $\partial \cdot / \partial n_i$  denotes the outer normal derivative with respect to  $\Omega_i$ ,  $i = 1, 2$ . The scalar valued coefficient function  $\beta$  is assumed to be constant on each subdomain, namely,  $\beta = \beta_i$  in  $\Omega_i$ ,  $i = 1, 2$ , where  $\beta_1$  and  $\beta_2$  are two positive constants. Finally,  $f$  is assumed to be in  $L^2(\Omega)$ .

In the rest of this section, we introduce some preliminary results, the assumption on our triangulation and the finite element space. For  $s \geq 0$  and a Lipschitz domain  $\omega$ , we denote by  $H^s(\omega)$  the standard Sobolev space (see, e.g., [1]); the space  $H_0^1(\Omega)$  is the subspace of  $H^1(\Omega)$  consisting of all functions that vanish on  $\partial\Omega$  in the sense of traces. For simplicity of notation, we also identify  $L^2(\Omega)$  and  $H^0(\Omega)$  and the corresponding symbols for the norms. We also employ the Besov space  $B_{2,1}^{1/2}(\omega) := (L^2(\omega), H^1(\omega))_{1/2,1}$ , which is defined by interpolation using the “real method” [25,26]. We mention the important fact that for every  $\varepsilon > 0$  we have the embeddings  $H^{1/2+\varepsilon}(\omega) \subset B_{2,1}^{1/2}(\omega) \subset H^{1/2-\varepsilon}(\omega)$ . Finally, for the set  $\Omega_1 \cup \Omega_2$ , the space  $H^s(\Omega_1 \cup \Omega_2)$  denotes the space of all functions  $u$  with  $u|_{\Omega_i} \in H^s(\Omega_i)$  for  $i \in \{1, 2\}$ . This space is endowed with the norm  $\|u\|_{H^s(\Omega_1 \cup \Omega_2)}^2 := \|u\|_{H^s(\Omega_1)}^2 + \|u\|_{H^s(\Omega_2)}^2$ . Finally, the Besov space  $B_{2,1}^{1/2}(\Omega_1 \cup \Omega_2)$  is defined analogously, and we set  $\|u\|_{B_{2,1}^{1/2}(\Omega_1 \cup \Omega_2)}^2 := \|u\|_{B_{2,1}^{1/2}(\Omega_1)}^2 + \|u\|_{B_{2,1}^{1/2}(\Omega_2)}^2$ .

For non-negative expressions  $A, B$ , the notation  $A \lesssim B$  means the existence of a generic constant  $C > 0$  such that  $A \leq CB$ , where  $C$  is independent of relevant parameters (e.g., the mesh size).

Of special interest in our analysis are tubular neighborhoods  $S_\delta$  of the interface  $\Gamma$  of width  $2\delta > 0$  defined by

$$S_\delta := \{x \in \Omega; \text{dist}(x, \Gamma) < \delta\}.$$

We have the following result:

**Lemma 2.1.** For  $z \in B_{2,1}^{1/2}(\Omega_1 \cup \Omega_2)$ , we have

$$\|z\|_{L^2(S_\delta)}^2 \lesssim \delta \|z\|_{B_{2,1}^{1/2}(\Omega_1 \cup \Omega_2)}^2, \quad (3)$$

and for  $z \in H^t(\Omega_1 \cup \Omega_2)$  with  $t \in [0, \frac{1}{2})$ , we get

$$\|z\|_{L^2(S_\delta)} \lesssim \delta^t \|z\|_{H^t(\Omega_1 \cup \Omega_2)}. \quad (4)$$

Furthermore, for  $z \in H^1(\Omega)$  with  $z|_{\Gamma} = 0$  there holds

$$\|z\|_{L^2(S_{2\delta})} \lesssim \delta \|\nabla z\|_{L^2(S_{2\delta})}. \quad (5)$$

**Proof.** For the bound (3), we start with the 1D Gagliardo–Nirenberg inequality  $\|z\|_{L^\infty(I)}^2 \leq C \|z\|_{L^2(I)} \|z\|_{H^1(I)}$ , where  $I$  is a fixed interval. For arbitrary  $t > 0$ , we then get  $\|z\|_{L^\infty(I)}^2 \leq Ct \|z\|_{L^2(I)}^2 + Ct^{-1} \|z\|_{H^1(I)}^2$ . If the interface  $\Gamma$  is perfectly flat and may be viewed as a subset of  $\mathbb{R}^{d-1}$ , then we can infer from this for  $i \in \{1, 2\}$

$$\|z\|_{L^2(S_\delta \cap \Omega_i)}^2 \leq C \delta [t \|z\|_{L^2(\Omega_i)}^2 + t^{-1} \|z\|_{H^1(\Omega_i)}^2]. \quad (6)$$

Since Sobolev spaces are invariant under smooth changes of variables, we see that (6) is true without the assumption that  $\Gamma$  is perfectly flat. Selecting  $t = \|z\|_{H^1(\Omega_i)} / \|z\|_{L^2(\Omega_i)}$  in (6) (the case  $\|z\|_{L^2(\Omega_i)} = 0$  is an easy special case) we arrive at

$$\|z\|_{L^2(S_\delta \cap \Omega_i)}^2 \leq C \delta \|z\|_{L^2(\Omega_i)} \|z\|_{H^1(\Omega_i)} \quad \forall z \in H^1(\Omega_i).$$

From [25, Lemma 25.3] we then infer  $\|z\|_{L^2(S_\delta \cap \Omega_i)} \leq C \sqrt{\delta} \|z\|_{B_{2,1}^{1/2}(\Omega_i)}$ . Thus, (3) is proved.

The bound (4) follows from an interpolation argument: If  $\chi_{S_\delta \cap \Omega_i}$  denotes the characteristic function for the set  $S_\delta \cap \Omega_i$ , then the linear map  $L_\delta : z \mapsto \chi_{S_\delta \cap \Omega_i} z$  satisfies trivially  $\|L_\delta z\|_{L^2(\Omega_i)} \leq \|z\|_{L^2(\Omega_i)}$  and  $\|L_\delta z\|_{L^2(\Omega_i)} \lesssim \sqrt{\delta} \|z\|_{B_{2,1}^{1/2}(\Omega_i)}$  by (3). Since, by the reiteration theorem, we have for  $t \in (0, 1/2)$  the interpolation representation  $H^t(\Omega_i) = (L^2(\Omega_i), B_{2,1}^{1/2}(\Omega_i))_{2t,2}$ , the estimate  $\|z\|_{L^2(S_\delta \cap \Omega_i)} \leq C \delta^t \|z\|_{H^t(\Omega_i)}$  follows by an interpolation argument. This proves (4).

Finally, the bound (5) also follows from a 1D Sobolev embedding theorem by observing that for univariate functions  $z$  the condition  $z(0) = 0$  implies  $|z(x)|^2 = |\int_0^x z'(t) dt|^2 \leq |x| \|z'\|_{L^2(I)}^2$  for every  $x \in I$ .  $\square$

In addition to  $\delta$ -strip arguments, stable extensions play an important role in the subsequent analysis. For any function  $v$  defined on  $\Omega_i$ ,  $i = 1, 2$ , we will need an extension to  $\mathbb{R}^d$ . This can be achieved with the Stein extension operator  $E_i : L^2(\Omega_i) \rightarrow L^2(\mathbb{R}^d)$ , [23, Chapter VI.3, Theorem 5]. Without loss of generality we assume that  $E_1 v = 0$  on  $\partial\Omega$  for  $v \in H^1(\Omega_1)$ . We recall that this operator is a bounded linear operator for Sobolev and Besov spaces, e.g.,  $E_i : H^s(\Omega_i) \rightarrow H^s(\mathbb{R}^d)$  for any fixed  $s \geq 0$ .

## 2.1. Triangulations

We decompose the domain  $\Omega$  by a set  $\mathcal{T}_h$  of possibly curved open simplicial elements  $K$ . Each element  $K \in \mathcal{T}_h$  is the image of a standard open unit simplex, the so-called reference element  $\widehat{K} \subset \mathbb{R}^d$ , under an element mapping  $F_K : \widehat{K} \rightarrow K$ . In order to formulate condition (T3) in Definition 2.2 in a convenient fashion, we assume that the reference element  $\widehat{K}$  has congruent edges and faces (in 3D). For each element  $K$ , the images of faces, edges and vertices of the reference element  $\widehat{K}$  under the mapping  $F_K$  are called faces, edges, and vertices of  $K$ , respectively. We set  $2h_K := \text{diam } K$  and note that  $K \subset B_{h_K}(b_K)$ , where  $b_K$  is the barycenter of the element  $K$ . Here,  $B_r(x_c)$  denotes the ball of radius  $r$  centered at  $x_c$ . Let  $\rho_K$  be the maximal radius such that  $B_{\rho_K}(b_K) \subset K$  and define  $h := \min_{K \in \mathcal{T}_h} \rho_K$ .

In this paper we assume that the element mappings satisfy the definition of  $\gamma$ -shape regularity.

**Definition 2.2** ( $\gamma$ -shape regular). A triangulation  $\mathcal{T}_h$  with corresponding element mappings  $\{F_K\}_{K \in \mathcal{T}_h}$  is called a  $\gamma$ -shape regular triangulation of  $\Omega$  if the following conditions are satisfied:

- (T1) The mappings  $F_K : \widehat{K} \rightarrow K = F_K(\widehat{K})$  are  $C^1$ -diffeomorphisms between  $\widehat{K}$  and  $K$ .
- (T2)  $\overline{\Omega} = \bigcup_{K \in \mathcal{T}_h} \overline{K}$ ; and for all  $K, K' \in \mathcal{T}_h$  there holds either  $K = K'$  or  $K \cap K' = \emptyset$ .
- (T3) For each pair of elements  $K$  and  $K'$  from  $\mathcal{T}_h$ , the intersection  $\partial K \cap \partial K'$  is either empty, a face, an edge or a vertex shared by  $K$  and  $K'$ . If  $\sigma = \partial K \cap \partial K' \neq \emptyset$ , the mapping  $x \mapsto (F_K^{-1} \circ F_{K'})(x)$  is an isometric isomorphism between  $F_K^{-1}(\sigma)$  and  $F_{K'}^{-1}(\sigma)$ .
- (T4)  $\|DF_K\|_{L^\infty(\widehat{K})} \leq \gamma h_K$  and  $\|(DF_K)^{-1}\|_{L^\infty(\widehat{K})} \leq \gamma h_K^{-1}$  for all  $K \in \mathcal{T}_h$ , where  $DF_K$  is the Jacobian of  $F_K$ .

Examples of specific choices of suitable element mappings  $F_K$  will be discussed in Section 4. In addition to the shape regularity, we will restrict our analysis in this paper to quasi-uniform triangulations  $\mathcal{T}_h$ , i.e.,

$$h \leq h_K \lesssim h, \quad \forall K \in \mathcal{T}_h. \quad (7)$$

We point out that Condition T4 implies that the number of elements that share a node or an edge is bounded by a constant independent of  $h$ ; this constant depends solely on  $\gamma$ . Moreover, the  $\gamma$ -shape regularity of the triangulation  $\mathcal{T}_h$  and the quasi-uniformity of the mesh (7) ensure that, for each fixed  $r > 0$ , the number of balls  $B_{rh}(b_K)$  that overlap is bounded by an  $h$ -independent constant. Finally, there exist  $0 < r_0 < r_1 < \infty$  such that for all elements  $K$

$$K \subset B_{r_0 h}(b_K) \quad \text{and} \quad B_K := \bigcup_{x \in \widehat{K}} (B_h(x) \cap \Omega) \subset B_{r_1 h}(b_K).$$

## 2.2. Finite element spaces

Let  $P_p(D)$  be the space of polynomials on the  $d'$ -dimensional domain  $D$  of total degree less than or equal to  $p$  in  $d'$  variables. Then we define the finite element space

$$S^p(\mathcal{T}_h) = \{u \in H^1(\Omega); u|_K \circ F_K \in P_p(\widehat{K}) \quad \forall K \in \mathcal{T}_h\}$$

and its subspace  $S_0^p(\mathcal{T}_h) = S^p(\mathcal{T}_h) \cap H_0^1(\Omega)$ . The approximation theory of Section 3 will be based on a locally defined quasi-interpolation operator onto  $S_0^p(\mathcal{T}_h)$ . We recall that the simplicial reference element of order  $p$  is a triple  $(\widehat{K}, \widehat{\mathcal{E}}_p, P_p(\widehat{K}))$ , where  $\widehat{\mathcal{E}}_p = \{\hat{a}_i^p \in \widehat{K} \mid i = 1, \dots, N_p\}$  is a set of nodal points in  $\widehat{K}$ , with  $N_p = \dim P_p(\widehat{K})$ . For the sake of definiteness, we select for  $\widehat{\mathcal{E}}_p$  the classical equidistant arrangement given in [9, Formula 2.2.11, p. 49]. We will denote the standard nodal interpolation operator on the reference element  $\widehat{K}$  by  $\hat{I}_p : C(\widehat{K}) \rightarrow P_p(\widehat{K})$  and define  $I_p$  elementwise by

$$(I_p u)|_K = (\hat{I}_p(u|_K \circ F_K)) \circ F_K^{-1} \quad \forall K \in \mathcal{T}_h.$$

Condition T3 of Definition 2.2 explicitly requires the parametrizations from two neighboring elements to be the same on their common part and thus  $I_p : C(\overline{\Omega}) \rightarrow S^p(\mathcal{T}_h)$  is well-defined and  $(I_p u)|_{\partial\Omega} = 0$  if  $u|_{\partial\Omega} = 0$ . We set  $\mathcal{E}(\mathcal{T}_h) := \bigcup_{K \in \mathcal{T}_h} F_K(\widehat{\mathcal{E}}_p)$  and observe that each element  $v \in S^p(\mathcal{T}_h)$  is uniquely determined by specifying the nodal values at the nodes in  $\mathcal{E}(\mathcal{T}_h)$ .

To obtain optimal a priori estimates for a finite element solution, the associated finite element space has to satisfy suitable approximation properties. From now on, we assume that the following assumption on the element mappings holds.

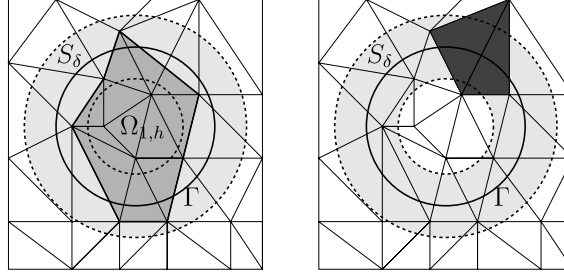


Fig. 2. A  $\delta$ -resolved interface (left) and a non- $\delta$ -resolved interface (right).

**Assumption 2.3.** The element mappings satisfy for all  $v \in H^{p+1}(K)$ :

$$h^{d/2} \|v - I_p v\|_{L^\infty(K)} + \sum_{l=0}^1 h^l \|v - I_p v\|_{H^l(K)} \lesssim h^{p+1} \|v\|_{H^{p+1}(K)}. \quad (8)$$

We note that Assumption 2.3 trivially holds for affine and isoparametric element mappings (cf. Ciarlet [9], Theorems 3.1.6, 4.3.4, and Example 4.3.8). Assumption 2.3 quantifies the approximation properties of the nodal interpolation operator  $I_p$  on each element  $K$  for rather smooth functions. To show suitable approximation properties of  $S_0^p(\mathcal{T}_h)$  in the space  $H^s(\Omega_1 \cup \Omega_2) \cap H_0^1(\Omega)$ ,  $s \in [1, p+1]$ , we construct in the next section a quasi-interpolation operator based on ideas from the classical Clément type operator [10] and from the boundary recovery techniques of a locally defined low order Scott–Zhang type operator [22]. We note that the present work is firmly rooted in the  $h$ -version context; that is, all constants do possibly depend on the polynomial degree  $p$ .

### 3. A quasi-interpolation operator

In this section, we study the approximation of piecewise smooth functions by finite elements in space  $S_0^p(\mathcal{T}_h)$ . Clearly the accuracy of this approximation depends on how well the mesh  $\mathcal{T}_h$  can resolve the interface  $\Gamma$ . In order to be able to quantify this approximation quality, we decompose, for  $\delta > 0$ , the triangulation  $\mathcal{T}_h$  into three disjoint subsets  $\mathcal{T}_h = \mathcal{T}_h^1 \cup \mathcal{T}_h^2 \cup \mathcal{T}_\star$ , where

$$\mathcal{T}_h^i = \{K \in \mathcal{T}_h; K \subset \Omega_i \setminus S_\delta\}, \quad i = 1, 2,$$

and  $\mathcal{T}_\star := \mathcal{T}_h \setminus (\mathcal{T}_h^1 \cup \mathcal{T}_h^2)$ . An element  $K \in \mathcal{T}_\star$  is called an interface element, and  $K \in \mathcal{T} \setminus \mathcal{T}_\star$  is called a non-interface element. Next, we set

$$\mathcal{T}_\star^i := \{K \in \mathcal{T}_\star; K \subset \Omega_i \cup S_\delta\}.$$

In general,  $\mathcal{T}_\star^1 \cap \mathcal{T}_\star^2$  may not be empty. However, an element  $K \in \mathcal{T}_\star^1 \cap \mathcal{T}_\star^2$  has to satisfy  $K \subset S_\delta$  and *a fortiori*  $B_h(b_K) \subset S_\delta$ , which implies  $h \leq \delta$ . Since the focus of our analysis is on small  $\delta$  ( $\delta = O(h^2)$  is a typical situation) we assume henceforth  $S_\delta \subset \Omega$  and

$$2\delta \leq h. \quad (9)$$

In this case,  $\mathcal{T}_\star^1 \cap \mathcal{T}_\star^2 = \emptyset$ . Furthermore, we are primarily interested in the case that the sets  $\mathcal{T}_\star^1$  and  $\mathcal{T}_\star^2$  make up the set  $\mathcal{T}_\star$ . This situation is formalized in the following definition:

**Definition 3.1** ( $\delta$ -resolved). The interface  $\Gamma$  is  $\delta$ -resolved by the triangulation  $\mathcal{T}_h$  if

$$\mathcal{T}_\star = \mathcal{T}_\star^1 \cup \mathcal{T}_\star^2 \quad \text{and} \quad \mathcal{T}_\star^1 \cap \mathcal{T}_\star^2 = \emptyset.$$

Fig. 2 illustrates Definition 3.1. On the left, the interface  $\Gamma$  is  $\delta$ -resolved by the triangulation  $\mathcal{T}_h$ , whereas this is not the case in the right picture. We note that the two shaded elements are in  $\mathcal{T}_\star$  but not in  $\mathcal{T}_\star^1 \cup \mathcal{T}_\star^2$ .

Associated with the decomposition of  $\mathcal{T}_h$  are approximations  $\Omega_{i,h}$  to the sets  $\Omega_i$  and an approximation  $\Gamma_h$  of the interface  $\Gamma$  given by

$$\bar{\Omega}_{i,h} := \bigcup \{\bar{K}; K \in \mathcal{T}_h^i \cup \mathcal{T}_\star^i\}, \quad \Gamma_h := \partial \Omega_{1,h}. \quad (10)$$

An important observation is that for  $\delta$ -resolved interfaces the approximate interface  $\Gamma_h$  is contained in  $S_\delta$ :

$$\Gamma_h \subset S_\delta. \quad (11)$$

**Example 3.2.** Let  $\Gamma$  be of class  $C^2$  and let  $\mathcal{T}_h$  be an *affine* triangulation with the property that for each element  $K$  all its  $d+1$  nodes are completely contained in either  $\overline{\Omega}_1$  or  $\overline{\Omega}_2$ . Then the interface  $\Gamma$  is  $O(h^2)$ -resolved by the mesh.

Next, we define the quasi-interpolation operator  $Q$ . This operator coincides with a standard Clément type quasi-interpolation operator on any non-interface interior element in  $\mathcal{T}_h^i$ ,  $i = 1, 2$ , and is an appropriate modification of the Scott–Zhang operators [22], for interface  $\mathcal{T}_\star^i$  and boundary elements. Before formally introducing this operator in Definition 3.3, we need some notation:

For  $\xi \in \mathcal{E}(\mathcal{T}_h) \cap \Omega_{i,h}$ , let  $\Pi_\xi$  be the  $L^2$ -projection onto  $P_p(B_h(\xi) \cap \Omega_i)$ . We emphasize that  $\xi$  is not necessarily contained in  $B_h(\xi) \cap \Omega_i$ . However, the condition  $2\delta \leq h$  guarantees that  $B_h(\xi) \cap \Omega_i$  contains a ball of radius  $\gtrsim h$ .

For  $\xi \in \mathcal{E}(\mathcal{T}_h) \cap \Gamma_h$  or  $\xi \in \mathcal{E}(\mathcal{T}_h) \cap \partial\Omega$ , there exists an element  $K_\xi$  and a face  $\sigma_\xi \subset \partial K_\xi$ , not necessarily unique, with  $\xi \in \overline{\sigma_\xi} \subset (\partial\Omega \cup \Gamma_h)$ . We select one such element  $K_\xi$  and denote by  $\hat{\sigma}_\xi$  the face of  $\hat{K}$  with  $F_{K_\xi}(\hat{\sigma}_\xi) = \sigma_\xi$ . We denote by  $\hat{\pi}_\xi$  the  $L^2$ -projection onto  $P_p(\hat{\sigma}_\xi)$ . In this setting, we employ the notation  $\hat{v}_\xi := v \circ F_{K_\xi}$  and set  $\hat{\xi} := F_{K_\xi}^{-1}(\xi) \in \hat{\mathcal{E}}_p$ .

We are now able to define the quasi-interpolation operator  $Q$ :

**Definition 3.3** (Quasi-interpolation). Let  $\Gamma$  be  $\delta$ -resolved by  $\mathcal{T}_h$ , and let  $S^p(\mathcal{T}_h)$  be the space defined in (2.2). The operator  $Q : H^1(\Omega) \rightarrow S^p(\mathcal{T}_h)$  is defined by specifying its nodal values:

$$Qv(\xi) := \begin{cases} \Pi_\xi v(\xi), & \xi \in \mathcal{E}(\mathcal{T}_h) \cap \Omega_{i,h}, i = 1, 2, \\ \hat{\pi}_\xi \hat{v}_\xi(\hat{\xi}), & \xi \in \mathcal{E}(\mathcal{T}_h) \cap (\partial\Omega \cup \Gamma_h). \end{cases}$$

We note that  $Q$  preserves homogeneous Dirichlet boundary conditions, and for  $v \in L^2(\Omega)$  with  $v|_{B_K} \in P_p(B_K)$  we have  $Qv|_K = I_p v|_K$  if  $\partial K \cap (\partial\Omega \cup \partial\Omega_{1,h}) = \emptyset$ . Before we focus on the approximation property of  $Q$ , we consider its stability.

**Lemma 3.4.** Under Assumption 2.3, the operator  $Q$  has the following local stability property for  $v \in H^1(\Omega)$  and  $i \in \{1, 2\}$ :

$$\|Qv\|_{L^2(K)} \lesssim \begin{cases} \|v\|_{L^2(B_K \cap \Omega_i)} & \text{for } K \in \mathcal{T}_h^i \text{ s.t. } \bar{K} \cap \partial\Omega = \emptyset; \\ \|v\|_{L^2(B_K \cap \Omega_i)} + h\|\nabla v\|_{L^2(\omega_K)} & \text{for } K \in \mathcal{T}_h^i \text{ s.t. } \bar{K} \cap \partial\Omega \neq \emptyset; \\ \|v\|_{L^2(B_K \cap \Omega_i)} + \sqrt{\frac{h}{\delta}}\|v\|_{L^2(\omega_K \cap S_{2\delta})} + \sqrt{h\delta}\|\nabla v\|_{L^2(\omega_K \cap S_{2\delta})} & \text{for } K \in \mathcal{T}_\star^i, \end{cases}$$

where

$$\omega_K := \bigcup_{K' \in \mathcal{T}_h: \bar{K}' \cap \bar{K} \neq \emptyset} K'.$$

**Proof.** Since the procedure is quite standard for all elements  $K$  that are not in the set  $\mathcal{T}_\star^1 \cup \mathcal{T}_\star^2$ , we restrict our attention to the case  $K \in \mathcal{T}_\star^i$ . We start with the following observation: If  $\hat{\sigma}_\xi$  is a face of the reference element  $\hat{K}$  and if we set  $\hat{S}_{\delta'} := \{x \in \hat{K}; \text{dist}(\hat{\sigma}_\xi, x) < \delta'\}$ , then

$$\|\hat{v}\|_{L^2(\hat{\sigma}_\xi)} \lesssim \frac{1}{\sqrt{\delta'}} \|\hat{v}\|_{L^2(\hat{S}_{\delta'})} + \sqrt{\delta'} \|\nabla \hat{v}\|_{L^2(\hat{S}_{\delta'})}, \quad (12)$$

where the hidden constant is independent of  $\delta' > 0$ .

Using the local volume and surface  $L^2$ -stability of  $\Pi_\xi$  and  $\hat{\pi}_\xi$ , respectively, we find with Assumption 2.3 for  $K \in \mathcal{T}_\star^i$

$$\begin{aligned} \|Qv\|_{L^2(K)}^2 &\lesssim h^d \sum_{\xi \in \mathcal{E}(K)} Qv(\xi)^2 \\ &\lesssim h^d \sum_{\xi \in \mathcal{E}(K) \setminus \Gamma_h} \Pi_\xi v(\xi)^2 + h^d \sum_{\xi \in \mathcal{E}(K) \cap \Gamma_h} \hat{\pi}_\xi \hat{v}_\xi(\hat{\xi})^2 \\ &\lesssim \|v\|_{L^2(B_K \cap \Omega_i)}^2 + h^d \sum_{\xi \in \mathcal{E}(K) \cap \Gamma_h} \|\hat{v}_\xi\|_{L^2(\hat{\sigma}_\xi)}^2 \\ &\lesssim \|v\|_{L^2(B_K \cap \Omega_i)}^2 + h^d \sum_{\xi \in \mathcal{E}(K) \cap \Gamma_h} \left( \frac{1}{\delta'} \|\hat{v}_\xi\|_{L^2(\hat{S}_{\delta'})}^2 + \delta' \|\nabla \hat{v}_\xi\|_{L^2(\hat{S}_{\delta'})}^2 \right) \\ &\lesssim \|v\|_{L^2(B_K \cap \Omega_i)}^2 + \frac{1}{\delta'} \|v\|_{L^2(\omega_K \cap S_{\delta+c\delta'h})}^2 + h^2 \delta' \|\nabla v\|_{L^2(\omega_K \cap S_{\delta+c\delta'h})}^2, \end{aligned}$$

where the constant  $c > 0$  depends solely on the shape-regularity of the triangulation. Here, we exploited the fact that for  $\xi \in \mathcal{E}(K) \cap \Gamma_h$  the selected face  $\sigma_\xi$  satisfies  $\sigma_\xi \subset \Gamma_h \subset S_\delta$ . Choosing  $\delta' = \delta/(ch)$  gives the desired bound.  $\square$

We observe that by setting  $\delta' = 1$  in the proof of Lemma 3.4, we get

$$\|Qv\|_{L^2(K)} \lesssim \|v\|_{L^2(B_K)} + h\|v\|_{H^1(B_K)}. \quad (13)$$

**Theorem 3.5.** Let  $d \in \{2, 3\}$ , assume (9), and let  $Q$  be the quasi-interpolation introduced in Definition 3.3. Assume that the nodal interpolation operator  $I_p$  satisfies Assumption 2.3. Let  $s \in [1, p+1]$ . Then  $Qu \in S_0^p(\mathcal{T}_h)$  for all  $u \in H_0^1(\Omega)$ , and the following error bounds are true:

- If  $s \in [1, \frac{3}{2})$  there holds for all  $u \in H^1(\Omega) \cap H^s(\Omega_1 \cup \Omega_2)$ :

$$\|u - Qu\|_{L^2(\Omega)}^2 + h^2\|u - Qu\|_{H^1(\Omega)}^2 \lesssim h^{2s}\|u\|_{H^s(\Omega_1 \cup \Omega_2)}^2. \quad (14)$$

- If  $s \in [\frac{3}{2}, p+1]$  there holds for all  $u \in H^1(\Omega) \cap H^s(\Omega_1 \cup \Omega_2)$  with  $\nabla u \in B_{2,1}^{1/2}(\Omega_1 \cup \Omega_2)$

$$\|u - Qu\|_{L^2(\Omega)}^2 \lesssim h^{2s}\|u\|_{H^s(\Omega_1 \cup \Omega_2)}^2 + h\delta^2\|\nabla u\|_{B_{2,1}^{1/2}(\Omega_1 \cup \Omega_2)}^2, \quad (15)$$

$$\|u - Qu\|_{H^1(\Omega)}^2 \lesssim h^{2(s-1)}\|u\|_{H^s(\Omega_1 \cup \Omega_2)}^2 + \delta\|\nabla u\|_{B_{2,1}^{1/2}(\Omega_1 \cup \Omega_2)}^2, \quad (16)$$

$$\|u - Qu\|_{H^1(\Omega \setminus S_\delta)}^2 \lesssim h^{2(s-1)}\|u\|_{H^s(\Omega_1 \cup \Omega_2)}^2 + \delta\frac{\delta}{h}\|\nabla u\|_{B_{2,1}^{1/2}(\Omega_1 \cup \Omega_2)}^2. \quad (17)$$

**Proof.** Before proving the result, we point out that for  $s > 3/2$  the bounds (15)–(17) can be simplified by observing  $\|\nabla u\|_{B_{2,1}^{1/2}(\Omega_1 \cup \Omega_2)} \leq C\|u\|_{H^s(\Omega_1 \cup \Omega_2)}$ .

**Step 1:** Let  $s \in \{1, \dots, p+1\}$  and  $v \in H^s(\Omega)$ . For  $K \in \mathcal{T}_h$  let  $\omega_B$  be a ball of radius  $O(h)$  with  $B_K \cup \omega_K \subset \omega := \Omega \cap \omega_B$ . Then we claim

$$h^l\|v - Qv\|_{H^l(K)} \lesssim h^s\|v\|_{H^s(\omega)}, \quad l = 0, 1. \quad (18)$$

To see this, recall that by standard approximation results (see, e.g., [5, Lemma 4.3.8]), there exists a polynomial  $q_K$  of degree  $p$  such that the following approximation and stability properties are satisfied:

$$\|v - q_K\|_{L^2(\omega)} + h\|v - q_K\|_{H^1(\omega)} \lesssim h^s|v|_{H^s(\omega)}, \quad \|q_K\|_{H^s(\omega)} \lesssim \|v\|_{H^s(\omega)}. \quad (19)$$

Using the upper bounds (13) and (19) and an inverse estimate, we find for  $l = 0, 1$

$$\begin{aligned} h^l\|v - Qv\|_{H^l(K)} &\leq h^l(\|v - q_K\|_{H^l(K)} + \|Q(v - q_K)\|_{H^l(K)} + \|q_K - Qq_K\|_{H^l(K)}) \\ &\lesssim h^s|v|_{H^s(\omega)} + h^{p+1}\|q_K\|_{H^{p+1}(\omega)} + h^{d/2} \sum_{\xi \in \mathcal{E}_M(K)} |q_K(\xi) - Qq_K(\xi)| \\ &\lesssim h^s|v|_{H^s(\omega)} + h^s\|q_K\|_{H^s(\omega)} + h^{d/2} \sum_{\xi \in \mathcal{E}_M(K)} |q_K(\xi) - Qq_K(\xi)| \end{aligned} \quad (20)$$

with  $\mathcal{E}_M(K) := \{\xi \in \mathcal{E}(\mathcal{T}_h) \cap \partial K \cap (\partial\Omega \cup \Gamma_h)\}$ . Here, we have used Assumption 2.3, the observation that for polynomials  $p_K$  and interior nodes  $\xi \in \mathcal{E}(\mathcal{T}_h) \cap (\Omega_{1,h} \cup \Omega_{2,h})$ , we have  $I_p p_K(\xi) = Qp_K(\xi)$ . For fixed  $\xi \in \mathcal{E}_M(K)$  recall that we denote by  $\sigma_\xi$  the face that is used in the definition of the nodal value of  $Q$  at  $\xi$ . Using the fact that  $\hat{\pi}_\xi$  reproduces polynomials, we get (denoting  $\hat{q}_K$  the pull-back of  $q_K$  to  $\hat{K}$  with the element map  $F_{K_\xi}$ ):

$$\begin{aligned} |q_K(\xi) - (Qq_K)(\xi)| &\leq |q_K(\xi) - Iq_K(\xi)| + |\hat{I}_p \hat{q}_K(\hat{\xi}) - (\hat{\pi}_\xi \hat{q}_K)(\hat{\xi})| \\ &= |q_K(\xi) - Iq_K(\xi)| + |\hat{\pi}_\xi(\hat{I}_p \hat{q}_K)(\hat{\xi}) - (\hat{\pi}_\xi \hat{q}_K)(\hat{\xi})| \lesssim \|q_K - Iq_K\|_{L^\infty(\sigma_\xi)} \\ &\lesssim \|q_K - Iq_K\|_{L^\infty(K_\xi)} \leq Ch^{p+1-d/2}\|q_K\|_{H^{p+1}(K_\xi)} \leq Ch^{s-d/2}\|q_K\|_{H^s(\omega)}. \end{aligned}$$

This completes the proof of (18).

**Step 2:** By summation, we conclude for  $s \in \{1, \dots, p+1\}$ ,  $l \in \{0, 1\}$ , and  $i \in \{1, 2\}$  from (18) that

$$\begin{aligned} \|u - Qu\|_{H^l(\Omega)} &\lesssim h^{s-l}\|u\|_{H^s(\Omega)} \quad \forall u \in H^s(\Omega), \\ \|u - Qu\|_{H^l(\cup_{K \in \mathcal{T}_h^i} K)} &\lesssim h^{s-l}\|u\|_{H^s(\Omega_i)} \quad \forall u \in H^s(\Omega_i). \end{aligned}$$

Interpolation then allows us to extend these estimates to non-integers, i.e., for  $s \in [1, p+1]$  and  $l \in \{0, 1\}$  there holds

$$\|u - Qu\|_{H^l(\Omega)} \lesssim h^{s-l}\|u\|_{H^s(\Omega)} \quad \forall u \in H^s(\Omega), \quad (21)$$

$$\|u - Qu\|_{H^l(\cup_{K \in \mathcal{T}_h^i} K)} \lesssim h^{s-l}\|u\|_{H^s(\Omega_i)} \quad \forall u \in H^s(\Omega_i). \quad (22)$$

**Step 3:** We now prove the bounds for  $\|u - Qu\|_{H^l(\Omega)}$  for the case  $u \in H^s(\Omega_1 \cup \Omega_2)$  for  $s \in [3/2, p+1]$  together with the assumption  $\nabla u \in B_{2,1}^{1/2}(\Omega_1 \cup \Omega_2)$ . To that end, we write

$$\|u - Qu\|_{H^l(\Omega)}^2 = \sum_{i=1}^2 \sum_{K \in \mathcal{T}_h^i} \|u - Qu\|_{H^l(K)}^2 + \sum_{i=1}^2 \sum_{K \in \mathcal{T}_*^i} \|u - Qu\|_{H^l(K)}^2.$$

The first sum is bounded by  $h^{2(s-l)} \|u\|_{H^s(\Omega_1 \cup \Omega_2)}^2$  in view of (22). Using the stability result of Lemma 3.4 and an inverse estimate for the elements in  $S^p(\mathcal{T}_h)$ , we find for  $K \in \mathcal{T}_*^i$

$$\begin{aligned} h^l \|u - Qu\|_{H^l(K)} &\leq h^l \|u - E_i u\|_{H^l(K)} + h^l \|E_i u - Q E_i u\|_{H^l(K)} + h^l \|Q(E_i u - u)\|_{H^l(K)} \\ &\lesssim h^l \|u - E_i u\|_{H^l(K)} + h^l \|E_i u - Q E_i u\|_{H^l(K)} \\ &\quad + \sqrt{\frac{h}{\delta}} \|u - E_i u\|_{L^2(\omega_K \cap S_{2\delta})} + \sqrt{\delta h} \|u - E_i u\|_{H^1(\omega_K \cap S_{2\delta})}. \end{aligned} \quad (23)$$

The stability of  $E_i$  together with (21) implies

$$\sum_{i=1}^2 \sum_{K \in \mathcal{T}_*^i} h^{2l} \|E_i u - Q E_i u\|_{H^l(K)}^2 \lesssim h^{2s} \sum_{i=1}^2 \|E_i u\|_{H^s(\Omega_i)}^2 \lesssim h^{2s} \|u\|_{H^s(\Omega_1 \cup \Omega_2)}^2. \quad (24)$$

In view of Lemma 2.1 and the fact that  $(u - E_i u)|_\Gamma = 0$ , we can bound  $E_i u - u$  in the  $L^2$ -norm and the  $H^1$ -norm on  $S_{2\delta}$  by

$$\begin{aligned} \sum_{K \in \mathcal{T}_*^i} \|u - E_i u\|_{L^2(\omega_K \cap S_{2\delta})}^2 &\lesssim \|u - E_i u\|_{L^2(S_{2\delta})}^2 \lesssim \delta^2 \|\nabla u\|_{L^2(S_{2\delta})}^2 \lesssim \delta^3 \|\nabla u\|_{B_{2,1}^{1/2}(\Omega_1 \cup \Omega_2)}^2, \\ \sum_{K \in \mathcal{T}_*^i} \|u - E_i u\|_{H^1(\omega_K \cap S_{2\delta})}^2 &\lesssim \|u - E_i u\|_{H^1(S_{2\delta})}^2 \lesssim \delta \|\nabla u\|_{B_{2,1}^{1/2}(\Omega_i)}^2. \end{aligned}$$

Summing over all elements in  $\mathcal{T}_*$ , observing  $E_i u = u$  on  $\Omega_i$  and using  $2\delta \leq h$ , we get

$$\begin{aligned} \sum_{i=1}^2 \sum_{K \in \mathcal{T}_*^i} \|u - Qu\|_{L^2(K)}^2 &\lesssim h^{2s} \|u\|_{H^s(\Omega_1 \cup \Omega_2)}^2 + h\delta^2 \|\nabla u\|_{B_{2,1}^{1/2}(\Omega_1 \cup \Omega_2)}^2, \\ \sum_{i=1}^2 \sum_{K \in \mathcal{T}_*^i} \|u - Qu\|_{H^1(K)}^2 &\lesssim h^{2(s-1)} \|u\|_{H^s(\Omega_1 \cup \Omega_2)}^2 + \delta \|\nabla u\|_{B_{2,1}^{1/2}(\Omega_1 \cup \Omega_2)}^2. \end{aligned}$$

This gives (14) and (15). We finally consider the error estimate in the  $H^1(\Omega \setminus S_\delta)$ -norm. This case can be handled in the same way as the  $H^1(\Omega)$ -estimate. The only difference is to replace  $K$  by  $K \setminus S_\delta$  in (23) and observing that  $\|u - E_i u\|_{H^l(K \setminus S_\delta)} = 0$ .

**Step 4:** It remains to bound  $\|u - Qu\|_{H^l(\Omega)}$  for the case  $u \in H^s(\Omega_1 \cup \Omega_2)$  for  $1 \leq s < 3/2$ . We proceed as in Step 3. The estimate (24) is immediately valid. For  $\sum_{K \in \mathcal{T}_*^i} \|u - E_i u\|_{H^l(K)}$  we estimate as in Step 3

$$\begin{aligned} \sum_{K \in \mathcal{T}_*^i} \|u - E_i u\|_{L^2(\omega_K \cap S_{2\delta})}^2 &\lesssim \|u - E_i u\|_{L^2(S_{2\delta})}^2 \lesssim \delta^2 \|\nabla u\|_{L^2(S_{2\delta})}^2 \lesssim \delta^2 \delta^{2(s-1)} \|u\|_{H^s(\Omega_1 \cup \Omega_2)}^2, \\ \sum_{K \in \mathcal{T}_*^i} \|u - E_i u\|_{H^1(\omega_K \cap S_{2\delta})}^2 &\lesssim \|u - E_i u\|_{H^1(S_{2\delta})}^2 \lesssim \delta^{2(s-1)} \|u\|_{H^s(\Omega_1 \cup \Omega_2)}^2. \end{aligned}$$

Recalling the assumption  $\delta \leq 2h$  allows us to conclude the desired bounds.  $\square$

**Remark 3.6.** We note that if  $\delta = O(h^{p+1})$  then we obtain optimal estimates in the  $L^2$ - and in the  $H^1(\Omega \setminus S_\delta)$ -norm if  $u$  is sufficiently smooth. This is not the case for  $p > 1$  and the  $H^1(\Omega)$ -norm.

#### 4. Convergence analysis of finite element methods

In this section, we formulate the finite element approximation of the interface problem (1)–(2) and establish a priori error estimates.



#### 4.1. Finite element approximation

By integration by parts one can immediately derive the following weak formulation of the interface problem (1)–(2):

**Problem (P).** Find  $u \in H_0^1(\Omega)$  such that

$$a(u, v) = L(v) \quad \forall v \in H_0^1(\Omega), \quad (25)$$

where the bilinear form  $a(\cdot, \cdot) : H_0^1(\Omega) \times H_0^1(\Omega) \rightarrow \mathbb{R}$  is defined by

$$a(u, v) := \sum_{i=1}^2 \int_{\Omega_i} \beta_i \nabla u_i \cdot \nabla v_i \, dx,$$

and the linear form  $L(v) : H_0^1(\Omega) \rightarrow \mathbb{R}$  by  $L(v) := \int_{\Omega} f v \, dx$ . We note that the evaluation of the entries of the stiffness matrix involving interface elements is not trivial in 3D if the mesh is not aligned with the interface. A much more convenient formulation is obtained by using the following approximate bilinear form  $a_h(\cdot, \cdot)$ :

$$a_h(u, v) := \sum_{i=1}^2 \int_{\Omega_{i,h}} \beta_i \nabla u \cdot \nabla v \, dx, \quad (26)$$

where  $\Omega_{i,h}$  is defined by (10). It is obvious that the bilinear form  $a_h(\cdot, \cdot)$  still preserves the coercivity, and that the bilinear form  $a^\Delta(\cdot, \cdot) := a(u, v) - a_h(u, v)$  satisfies

$$|a^\Delta(u, v)| \lesssim \|u\|_{H^1(S_\delta)} \|v\|_{H^1(S_\delta)}. \quad (27)$$

In terms of the simplified bilinear form in (26), we can now define our finite element method for the variational problem (P).

**Problem (P<sub>h</sub>).** Find  $u_h \in S_0^p(\mathcal{T}_h)$  such that

$$a_h(u_h, v) = L(v) \quad \forall v \in S_0^p(\mathcal{T}_h). \quad (28)$$

#### 4.2. A priori estimates

##### 4.2.1. Energy norm estimates

We first analyze the FEM-convergence in the energy norm:

**Theorem 4.1.** Let  $u$  and  $u_h$  be the solutions to the problems (25) and (28) respectively. Assume (9) and that  $I_p$  satisfies Assumption 2.3. Let  $u \in H_0^1(\Omega) \cap H^s(\Omega_1 \cup \Omega_2)$  for some  $s \in [1, p+1]$ .

- For  $s \in [1, \frac{3}{2})$  there holds

$$\|u - u_h\|_{H^1(\Omega)} \lesssim h^{s-1} \|u\|_{H^s(\Omega_1 \cup \Omega_2)}.$$

- For  $s \in [\frac{3}{2}, p+1]$  and  $\nabla u \in B_{2,1}^{1/2}(\Omega_1 \cup \Omega_2)$  there holds

$$\|u - u_h\|_{H^1(\Omega)} \lesssim h^{s-1} \|u\|_{H^s(\Omega_1 \cup \Omega_2)} + \sqrt{\delta} \|\nabla u\|_{B_{2,1}^{1/2}(\Omega_1 \cup \Omega_2)}.$$

**Proof.** The first lemma of Strang (see, e.g., [9, Theorem 4.1.1]) yields

$$\|u - u_h\|_{H^1(\Omega)} \lesssim \inf_{w \in S_0^p(\mathcal{T}_h)} \left\{ \|u - w\|_{H^1(\Omega)} + \sup_{v \in S_0^p(\mathcal{T}_h)} \frac{|a(w, v) - a_h(w, v)|}{\|v\|_{H^1(\Omega)}} \right\}.$$

Theorem 3.5 gives an upper bound for the approximation error by setting  $w = Qu$ . The consistency error can be estimated by

$$|a^\Delta(Qu, v)| \lesssim \|Qu\|_{H^1(S_\delta)} \|v\|_{H^1(S_\delta)} \lesssim (\|u\|_{H^1(S_\delta)} + \|u - Qu\|_{H^1(S_\delta)}) \|v\|_{H^1(\Omega)},$$

and thus we find  $\|u - u_h\|_{H^1(\Omega)} \lesssim \|u - Qu\|_{H^1(\Omega)} + \|u\|_{H^1(S_\delta)}$ . Now Lemma 2.1 and Theorem 3.5 yield the upper bound for the discretization error in the energy norm.  $\square$

**Remark 4.2.** Theorem 4.1 quantifies the effect of approximating the interface. The compact embedding  $H^{\frac{1}{2}+\epsilon}(\Omega_i) \subset B_{2,1}^{1/2}(\Omega_i)$ ,  $i = 1, 2$ , and  $\epsilon > 0$  allows us to replace  $\|\nabla u\|_{B_{2,1}^{1/2}(\Omega_1 \cup \Omega_2)}$  by  $\|u\|_{H^s(\Omega_1 \cup \Omega_2)}$  if  $s > 3/2$ . In order to achieve the optimal  $p$ -th order approximation with the finite element space  $S^p(\mathcal{T}_h)$  in the  $H^1$ -norm, one has to ensure  $\delta = O(h^{2p})$ .

#### 4.2.2. $L^2$ -estimates

As is standard,  $L^2$ -estimates are based on approximation problems for suitable dual problems. Hence, regularity assertions for these dual problems are required. We formulate these assertions as an assumption of “ $\tau$ -regularity” in Assumption 4.3 and point out that all generic constants in the sequel will additionally depend on  $\tau$ .

**Assumption 4.3.** ( $\tau$ -regularity) For  $f \in L^2(\Omega)$  the solution  $u$  of the elliptic boundary value problem (1)–(2) satisfies  $u \in H_0^1(\Omega) \cap H^\tau(\Omega_1 \cup \Omega_2)$  for some  $\tau > \frac{3}{2}$  together with the following a priori estimate:

$$\|u\|_{H^\tau(\Omega_1 \cup \Omega_2)} \leq C \|f\|_{L^2(\Omega)}. \quad (29)$$

**Remark 4.4.** Assumption 4.3 is satisfied with  $\tau = 2$ , e.g., if  $\Omega$  is convex or  $\partial\Omega$  is sufficiently smooth [8,21]. Moreover Assumption 4.3 is always satisfied in our situation of piecewise constant coefficient  $\beta$  for polygonal (2D) or polyhedral (3D) Lipschitz domains: The smoothness of  $\Gamma$  and  $f \in L^2(\Omega)$  implies by standard arguments that  $u \in H^2((\Omega_1 \cup \Omega_2) \cap \Omega_2')$  (see, e.g., [8]). For the  $H^{3/2}$ -regularity near  $\partial\Omega$ , let  $\chi$  be a smooth cut-off function with  $\chi \equiv 1$  on  $\Omega \setminus \overline{\Omega_1'}$  and  $\chi \equiv 0$  on an open neighborhood of  $\overline{\Omega_1'}$ . The function  $\tilde{u} := \chi u$  then satisfies  $-\Delta \tilde{u} \in L^2(\Omega)$  and coincides with  $u$  on  $\Omega \setminus \overline{\Omega_1'}$ . By [14, Remark 2.4.6] for the 2D case and by [14, Corollary 2.6.7] for the 3D case there exists  $\tau \in (3/2, 2]$  and  $C > 0$  (both depending solely on  $\Omega$ ) such that  $\tilde{u}$  satisfies  $\|\tilde{u}\|_{H^\tau(\Omega)} \leq C \|\Delta \tilde{u}\|_{L^2(\Omega)}$ . The argument is concluded by noting  $\|\Delta \tilde{u}\|_{L^2(\Omega)} \leq C \|f\|_{L^2(\Omega)}$ .

We start with a technical lemma to be used in the subsequent convergence analysis.

**Lemma 4.5.** *There exists a positive constant  $\mu$  independent of  $h$  such that*

$$\|w_h\|_{H^1(S_\delta)} \lesssim \sqrt{\frac{\delta}{h}} \|w_h\|_{H^1(S_{\mu h})} \quad \forall w_h \in S^p(\mathcal{T}).$$

**Proof.** The smoothness of the interface  $\Gamma$  and the shape regularity of the triangulation imply that  $\text{meas}(K \cap S_\delta) \lesssim h^{d-1} \delta$  for every  $K \in \mathcal{T}_h$ . Hence

$$\begin{aligned} \|w_h\|_{H^1(S_\delta)}^2 &\leq \sum_{K \in \mathcal{T}_h: K \cap S_\delta \neq \emptyset} \|w_h\|_{H^1(K \cap S_\delta)}^2 \lesssim \sum_{K \in \mathcal{T}_h: K \cap S_\delta \neq \emptyset} \delta h^{d-1} \|w_h\|_{W^{1,\infty}(K)}^2 \\ &\lesssim \sum_{K \in \mathcal{T}_h: K \cap S_\delta \neq \emptyset} \delta h^{d-1} h^{-d} \|w_h\|_{H^1(K)}^2 \lesssim \frac{\delta}{h} \|w_h\|_{H^1(S_{\mu h})}^2. \quad \square \end{aligned}$$

The  $L^2$ -norm estimates for  $u - u_h$  can be obtained by duality arguments. Theorem 4.6 below gives error estimates for the  $L^2$ -error of the FEM. We point out that the condition on  $\delta$  to obtain optimal a priori estimates in the  $L^2$ -norm are not as strong as for the  $H^1$ -norm. In particular, for  $p > 1$ , isoparametric elements lead to optimal rates in the  $L^2$ - but not in the  $H^1$ -norm. For example, isoparametric quadratic finite elements achieve optimal third order convergence in the  $L^2$ -norm but, in general, only order 1.5 in the energy norm.

**Theorem 4.6.** *Under the hypotheses of Theorem 4.1 and Assumption 4.3, we have  $\min\{s, \tau\} > 3/2$  and the following estimate holds:*

$$\|u - u_h\|_{L^2(\Omega)} \lesssim (\delta + h^{s-1} \sqrt{\delta} + h^{s+\tau-2}) \|u\|_{H^s(\Omega_1 \cup \Omega_2)}.$$

**Proof.** We point out that the smoothness of  $\Gamma$  implies by Assumption 4.3 that  $s > 3/2$ .

For the duality argument, we define  $w \in H_0^1(\Omega)$  and  $w_h \in S_0^p(\mathcal{T}_h)$  by

$$a(v, w) = (u - u_h, v)_{L^2(\Omega)} \quad \forall v \in H_0^1(\Omega),$$

$$a(v, w_h) = (u - u_h, v)_{L^2(\Omega)} \quad \forall v \in S_0^p(\mathcal{T}_h).$$

That is,  $w$  is the weak solution to the interface problem (1)–(2) with  $f$  given by  $u - u_h$ . Assumption 4.3 implies  $w \in H^\tau(\Omega_1 \cup \Omega_2)$  with the a priori bound  $\|w\|_{H^\tau(\Omega_1 \cup \Omega_2)} \lesssim \|u - u_h\|_{L^2(\Omega)}$ . We note that  $w_h \in S_0^p(\mathcal{T}_h)$ , and thus Céa's Lemma can be applied yielding in view of Theorem 3.5

$$\begin{aligned} \|w - w_h\|_{H^1(\Omega)} &\lesssim \inf_{v \in S_0^p(\mathcal{T}_h)} \|w - v\|_{H^1(\Omega)} \leq \|w - Q w\|_{H^1(\Omega)} \\ &\lesssim (h^{\tau-1} + \sqrt{\delta}) \|w\|_{H^\tau(\Omega_1 \cup \Omega_2)} \lesssim (h^{\tau-1} + \sqrt{\delta}) \|u - u_h\|_{L^2(\Omega)}. \end{aligned} \quad (30)$$

Observing the Galerkin orthogonalities for  $w - w_h$  and  $e := u - u_h$

$$a(e, v) = -a^\Delta(u_h, v) \quad \forall v \in S_0^p(\mathcal{T}_h), \quad (31)$$

$$a(v, w - w_h) = 0 \quad \forall v \in S_0^p(\mathcal{T}_h), \quad (32)$$

gives

$$\begin{aligned} \|e\|_{L^2(\Omega)}^2 &= a(e, w) = a(e, w - w_h) + a(e, w_h) = a(u - Qu, w - w_h) - a^\Delta(u_h, w_h) \\ &\lesssim \|u - Qu\|_{H^1(S_\delta)} \|w - w_h\|_{H^1(S_\delta)} + \|u - Qu\|_{H^1(\Omega \setminus S_\delta)} \|w - w_h\|_{H^1(\Omega \setminus S_\delta)} \\ &\quad + \|u_h\|_{H^1(S_\delta)} \|w_h\|_{H^1(S_\delta)} =: T_1 + T_2 + T_3. \end{aligned}$$

Theorem 3.5 and (30) guarantees that  $T_2$  can be estimated in the desired way. Before we consider  $T_i$ ,  $i = 1, 3$ , in more detail, we bound  $\|u_h\|_{H^1(S_\delta)}$ ,  $\|w\|_{H^1(S_\delta)}$ , and  $\|w_h\|_{H^1(S_\delta)}$ . Applying Lemma 2.1 and Theorem 4.1, we find

$$\|u_h\|_{H^1(S_\delta)} \leq \|e\|_{H^1(S_\delta)} + \|u\|_{H^1(S_\delta)} \lesssim \|e\|_{H^1(\Omega)} + \sqrt{\delta} \|u\|_{H^s(\Omega_1 \cup \Omega_2)} \lesssim (\sqrt{\delta} + h^{s-1}) \|u\|_{H^s(\Omega_1 \cup \Omega_2)}.$$

Lemma 2.1 and the regularity Assumption 4.3 yield  $\|w\|_{H^1(S_\delta)} \lesssim \sqrt{\delta} \|e\|_{L^2(\Omega)}$ . To bound  $\|w_h\|_{H^1(S_\delta)}$ , we use Lemma 4.5 and (30)

$$\begin{aligned} \|w_h\|_{H^1(S_\delta)} &\lesssim \sqrt{\delta} h^{-1/2} \|w_h\|_{H^1(S_{\mu h})} \lesssim \sqrt{\delta} h^{-1/2} (\|w - w_h\|_{H^1(S_{\mu h})} + \|w\|_{H^1(S_{\mu h})}) \\ &\lesssim \sqrt{\delta} h^{-1/2} (\|w - w_h\|_{H^1(S_{\mu h})} + h^{1/2} \|w\|_{H^\tau(\Omega_1 \cup \Omega_2)}) \lesssim \sqrt{\delta} \|e\|_{L^2(\Omega)}. \end{aligned}$$

These preliminary results directly yield

$$T_1 + T_3 \lesssim (h^{s-1} + \sqrt{\delta}) \sqrt{\delta} \|e\|_{L^2(\Omega)} \|u\|_{H^s(\Omega_1 \cup \Omega_2)}. \quad \square$$

**Remark 4.7.** We note that for full regularity, i.e.,  $\tau = 2$ , the upper bound in Theorem 4.6 is  $O(\delta + h^s)$ . For  $\tau \in (\frac{3}{2}, 2)$ , the discretization error in the  $L^2$ -norm is at least  $O(\delta + h^{s-1/2})$ .

#### 4.3. Convergence away from the interface

As we will discuss in more detail in Theorem 4.12 below, the convergence result Theorem 4.1 does not lead to optimal convergence rates in the  $H^1(\Omega)$ -norm for isoparametric elements. In this section, we argue that this is due to the poor approximation within the tubular neighborhood  $S_\delta$  of the interface. Indeed, as it will be seen in Theorem 4.8 below, the condition  $\delta = O(h^{p+1})$  is sufficient to ensure optimal  $H^1$ -norm convergence of order  $O(h^p)$  in the region  $\Omega \setminus S_\delta$  away from the interface, as long as the exact solution  $u$  is sufficiently smooth in  $\Omega \setminus S_\delta$ .

**Theorem 4.8.** Under the hypotheses of Theorem 4.1 and Assumption 4.3, we have

$$\|u - u_h\|_{H^1(\Omega \setminus S_\delta)} \lesssim \left( h^{s-1} + \left( \frac{\delta}{h} \right)^{3/2} + \left( \frac{\delta}{h} \right) h^{1/4} + \left( \frac{\delta}{h} \right)^{1/2} (h^{s-3/2} + h^{(s-1)/2}) \right) \|u\|_{H^s(\Omega_1 \cup \Omega_2)}.$$

This leads to the optimal convergence rate when  $\delta = O(h^{\max\{2, s\}})$ :

$$\|u - u_h\|_{H^1(\Omega \setminus S_\delta)} \lesssim h^{s-1} \|u\|_{H^s(\Omega_1 \cup \Omega_2)}.$$

**Proof.** We denote by  $a_{h, \Omega \setminus S_\delta}(\cdot, \cdot)$  and  $a_{h, S_\delta}(\cdot, \cdot)$  the bilinear form obtained from (26) when the domain of integration is restricted to  $\Omega \setminus S_\delta$  and  $S_\delta$ , respectively. The Galerkin orthogonality (31) and the Cauchy–Schwarz inequality give us

$$\begin{aligned} |e|_{H^1(\Omega \setminus S_\delta)}^2 &\lesssim a_{h, \Omega \setminus S_\delta}(e, e) = a_h(e, e) - a_{h, S_\delta}(e, e) \\ &= a_h(e, u - Qu) - a^\Delta(e, Qu - u_h) - a_{h, S_\delta}(e, e) \\ &= a_{h, \Omega \setminus S_\delta}(e, u - Qu) - a^\Delta(e, Qu - u_h) - a_{h, S_\delta}(e, Qu - u_h) \\ &\lesssim |e|_{H^1(\Omega \setminus S_\delta)} \|u - Qu\|_{H^1(\Omega \setminus S_\delta)} + |e|_{H^1(S_\delta)} \|Qu - u_h\|_{H^1(S_\delta)}. \end{aligned}$$

Then we derive by using Young's inequality for the first term and the triangle inequality for the second term that

$$|e|_{H^1(\Omega \setminus S_\delta)}^2 \lesssim \|u - Qu\|_{H^1(\Omega \setminus S_\delta)}^2 + \|Qu - u_h\|_{H^1(S_\delta)}^2 + \|u - Qu\|_{H^1(S_\delta)} \|Qu - u_h\|_{H^1(S_\delta)}. \quad (33)$$

The error  $\|Qu - u_h\|_{H^1(S_\delta)}$  in (33) can be estimated with the aid of Lemma 4.5, Theorems 3.5 and 4.6, and Remark 4.7 as follows:

$$\begin{aligned}
\|Qu - u_h\|_{H^1(S_\delta)} &\lesssim \delta^{1/2} h^{-1/2} \|Qu - u_h\|_{H^1(S_{\mu h})} \lesssim \delta^{1/2} h^{-3/2} \|Qu - u_h\|_{L^2(S_{\mu h})} \\
&\lesssim \delta^{1/2} h^{-3/2} (\|Qu - u\|_{L^2(S_{\mu h})} + \|u - u_h\|_{L^2(S_{\mu h})}) \\
&\lesssim \delta^{1/2} h^{-3/2} (\delta + h^{s-1/2}) \|u\|_{H^s(\Omega_1 \cup \Omega_2)}.
\end{aligned} \tag{34}$$

Now Theorem 3.5 and (33) yield

$$|e|_{H^1(\Omega \setminus S_\delta)}^2 \lesssim \left\{ \frac{\delta^2}{h} + h^{2(s-1)} + \frac{\delta}{h^3} (\delta^2 + h^{2s-1}) + (\delta^{1/2} + h^{s-1}) \sqrt{\frac{\delta}{h^3}} (\delta + h^{s-1/2}) \right\} \|u\|_{H^s(\Omega_1 \cup \Omega_2)}^2,$$

which gives the desired result after rearranging terms and recalling  $\delta \leq 2h$ .  $\square$

The optimal  $H^1$ -convergence of Theorem 4.8 enables us to generalize a result from [3, Theorem 2.1]:

**Corollary 4.9.** *Let  $u$  and  $u_h$  be the solutions to the systems (25) and (28) respectively, and assume  $u \in H_0^1(\Omega) \cap H^{p+1}(\Omega_1 \cup \Omega_2)$ . Then under Assumption 4.3 the following estimate holds for  $\delta = O(h^{p+1})$ :*

$$\sum_{i=1}^2 \|\tilde{u}_i - u_h\|_{H^1(\Omega_{i,h})} \lesssim h^p \left( \sum_{i=1}^2 \|u\|_{H^{p+1}(\Omega_i)} + \|\tilde{u}_i\|_{H^{p+1}(\Omega)} \right).$$

Here,  $\tilde{u}_i \in H^{p+1}(\mathbb{R}^d)$  is any extension of the function  $u_i = u|_{\Omega_i}$  for  $i = 1, 2$ .

**Proof.** We will make use of two key observations in the following proof: first, for each  $K \in \mathcal{T}_h$ , there exists a fixed (open) ball  $\widehat{B} \subset \widehat{K}$  that is independent of  $h$  such that  $F_K(\widehat{B}) \subset K \setminus S_\delta$ ; this implies that  $\tilde{u}_i|_{F_K(\widehat{B})} = u|_{F_K(\widehat{B})}$  for each  $K \in \mathcal{T}_h^i \cup \mathcal{T}_\star^i$ . Second, all norms are equivalent on the finite-dimensional space of polynomials of degree  $p$ , in particular,  $\|\pi\|_{H^1(\widehat{K})} \sim \|\pi\|_{H^1(\widehat{B})}$  for all  $\pi \in \mathcal{P}_p(\widehat{K})$ .

For any  $K \in \mathcal{T}_h^i \cup \mathcal{T}_\star^i$ , we define  $\hat{u} := \tilde{u}_i|_K \circ F_K$ ,  $\hat{u} := u|_K \circ F_K$ ,  $\hat{u}_h := u_h|_K \circ F_K$ . Recalling the operator  $I_p$  of Section 2.2 and estimate (8), we derive for  $l \in \{0, 1\}$  that

$$\|\tilde{u}_i - u_h\|_{H^l(K)} \leq \|\tilde{u}_i - I_p \tilde{u}_i\|_{H^l(K)} + \|I_p \tilde{u}_i - u_h\|_{H^l(K)} \lesssim h^{p+1-l} \|\tilde{u}_i\|_{H^{p+1}(K)} + h^{d/2-l} \|\hat{I}_p \hat{u} - \hat{u}_h\|_{H^l(\widehat{K})}.$$

The second term above can be estimated further as follows:

$$\begin{aligned}
h^{d/2-l} \|\hat{I}_p(\hat{u} - \hat{u}_h)\|_{H^l(\widehat{K})} &\lesssim h^{d/2-l} \|\hat{I}_p(\hat{u} - \hat{u}_h)\|_{H^l(\widehat{B})} \\
&\leq h^{d/2-l} \|\hat{I}_p \hat{u} - \hat{u}\|_{H^l(\widehat{B})} + h^{d/2-l} \|\hat{u} - \hat{u}_h\|_{H^l(\widehat{B})} \\
&\lesssim \|I_p \tilde{u}_i - \tilde{u}_i\|_{H^l(K)} + \|\tilde{u}_i - u_h\|_{H^l(K \setminus S_\delta)} \\
&\lesssim \|I_p \tilde{u}_i - \tilde{u}_i\|_{H^l(K)} + \|u - u_h\|_{H^l(K \setminus S_\delta)} \\
&\lesssim h^{p+1-l} \|\tilde{u}_i\|_{H^{p+1}(K)} + \|u - u_h\|_{H^l(K \setminus S_\delta)}.
\end{aligned}$$

Now summing up both sides over all elements yields

$$\sum_{i=1}^2 \sum_{K \in \mathcal{T}_h^i \cup \mathcal{T}_\star^i} \|\tilde{u}_i - u_h\|_{H^l(K)}^2 \lesssim \sum_{i=1}^2 \sum_{K \in \mathcal{T}_h^i \cup \mathcal{T}_\star^i} h^{2(p+1-l)} \|\tilde{u}_i\|_{H^{p+1}(K)}^2 + \|u - u_h\|_{H^l(\Omega \setminus S_\delta)}^2.$$

The desired estimate now follows from selecting  $l = 1$  and appealing to Theorem 4.8.  $\square$

**Remark 4.10.** One possible choice of the extension  $\tilde{u}_i$  used in Corollary 4.9 is given by the Stein extension  $E_i u|_{\Omega_i}$ . Corollary 4.9 shows that the finite element approximation  $u_h$  is closer to  $E_i u|_{\Omega_i}$  on  $\Omega_{i,h}$  than to  $u$  in the case  $\delta = O(h^{p+1})$ . This improvement over Theorem 4.1 is achieved by changing the measurement of the error. This viewpoint was adopted in [3], where Corollary 4.9 was shown for the case that  $\Gamma$  is approximated by an interpolating spline of degree  $p$ . An alternative viewpoint is to ask whether it is possible to construct, by post-processing  $u_h$ , an approximation  $\tilde{u}_h$  that is closer to  $u$  on  $S_\delta$  than  $u_h$ . Indeed, it is possible to “extrapolate” the approximation  $u_h|_{\Omega \setminus S_\delta}$  to the tubular neighborhood  $S_\delta$  to arrive at a non-conforming approximation  $\tilde{u}_h$  ( $\tilde{u}_h$  is not necessarily in  $H^1(\Omega)$ ). This is the approach taken in [4] for the case  $p = 1$ .

#### 4.4. Applications and extensions

Theorems 4.1 and 4.6 quantify the convergence behavior of the finite element method in terms of the mesh size  $h$  and the parameter  $\delta$ , which measures how well the triangulation resolves the interface  $\Gamma$ . An important case of finite elements is that of *polynomial* element maps of degree  $m \in \mathbb{N}$ . The use of polynomial element maps results in a piecewise polynomial approximation of  $\Gamma$ ; hence, one expects  $\delta = O(h^{m+1})$ . We recall a standard terminology: the case  $m < p$  is referred to as *subparametric elements*, the case  $m = p$  as *isoparametric elements* and the case  $m > p$  as *superparametric elements*; see [5,9]. The construction of the element maps  $F_K$  was studied systematically in [17] in a way that not only Assumption 2.3 but also the approximation order of the interface  $\delta = O(h^{m+1})$  are satisfied.

**Remark 4.11.** Following [17, Lemma 5], one can show that if the interface  $\Gamma$  is of class  $C^{m+1}$  and if  $\mathcal{T}_h$  satisfies Definition 2.1, with all its element mappings  $F_K$  defined by  $m$ -th order polynomials (see [17] for details), then the interface  $\Gamma$  is  $O(h^{m+1})$ -resolved by  $\mathcal{T}_h$ .

Remark 4.11, along with Theorems 4.1, 4.6 and 4.8, implies the following convergence results:

**Theorem 4.12** (*Isoparametric and superparametric elements*). Let  $\Gamma$  be sufficiently smooth and the element mappings  $F_K$  be polynomials of degree  $m$  as constructed in [17]. Let  $u$  and  $u_h$  be the solutions to the systems (25) and (28), with  $u$  satisfying that  $u \in H^{p+1}(\Omega_1 \cup \Omega_2)$ . Then:

1. For isoparametric elements with  $m = p$ , there holds

$$\begin{aligned}\|u - u_h\|_{H^1(\Omega)} &\lesssim h^{(p+1)/2} \|u\|_{H^{p+1}(\Omega_1 \cup \Omega_2)}, \\ \|u - u_h\|_{H^1(\Omega \setminus S_\delta)} &\lesssim h^p \|u\|_{H^{p+1}(\Omega_1 \cup \Omega_2)},\end{aligned}$$

2. For superparametric elements with  $m \geq 2p - 1$ , there holds

$$\|u - u_h\|_{H^1(\Omega)} \lesssim h^p \|u\|_{H^{p+1}(\Omega_1 \cup \Omega_2)}.$$

If Assumption 4.3 is satisfied, then there holds in both cases additionally

$$\|u - u_h\|_{L^2(\Omega)} \lesssim h^{p+\tau-1} \|u\|_{H^{p+1}(\Omega_1 \cup \Omega_2)}.$$

**Remark 4.13.** Theorem 4.12 reveals that linear finite elements ( $m = p = 1$ ) indeed achieve optimal convergence order both in the  $H^1$ - and  $L^2$ -norms. While for higher order finite elements, isoparametric finite elements yield optimal convergence in the  $L^2$ -norm, but not in the  $H^1$ -norm. One has to resort to superparametric finite elements to recover the optimal convergence for the  $H^1$ -norm.

For the sake of exposition and clarity, we have chosen to avoid a few rather technical but practically important issues in the current work. Nevertheless, we believe that the theory of the present paper can be generalized in the following directions:

- *Piecewise smooth coefficients:* We have restricted our attention to piecewise constant coefficients  $\beta$  in (1). However, all our results can be extended to piecewise smooth coefficients. In this case, one needs to replace the constant  $\beta_i$  in (26) by some appropriate approximation of  $\beta|_K$ , e.g., an average or an interpolant of  $\beta$ .
- *Quasi-uniform triangulations:* The convergence theory has been established for quasi-uniform meshes (7). Conceivably, the analysis can be extended to more general, shape-regular triangulations with local mesh refinement. The assumption of quasi-uniformity, which is reasonable in the case of piecewise smooth solutions considered here, allows us to simplify covering arguments in the proofs of the a priori estimates. But all our operators are constructed locally, and thus our arguments can also be applied for locally quasi-uniform meshes.
- *Elasticity problems:* Using the vector-valued forms of the finite element spaces discussed in this work, one can solve elastic interface problems as well. Vectorized versions of the perturbed interpolation operator of Definition 3.3, the  $\delta$ -region argument of Lemma 2.1, and the approximation property of Theorem 3.5 can be derived analogously. In particular, for the simplest case with continuous piecewise linear finite elements with  $p = m = 1$ , vectorized version of Theorem 4.12 can be derived in a similar way. Optimal convergence rates, e.g., first order in the energy norm and second order in the  $L^2$ -norm, can readily be derived for the Lamé system.
- *Treatment of non-homogeneous interface source functions:* In our analysis, we have ignored variational crimes stemming from approximating the right-hand side  $L(\cdot)$ , which arises in particular when  $[\beta \partial u / \partial n] \neq 0$ . In this situation, a numerically feasible realization of  $L(\cdot)$  is likely to be based on the approximate interface  $\Gamma_h$ , which is a union of faces of elements. Then the error introduced by the approximation has to be quantified with techniques similar to [8] and the present paper provided that  $\Gamma_h$  and  $\Gamma$  are sufficiently close in an appropriate sense.

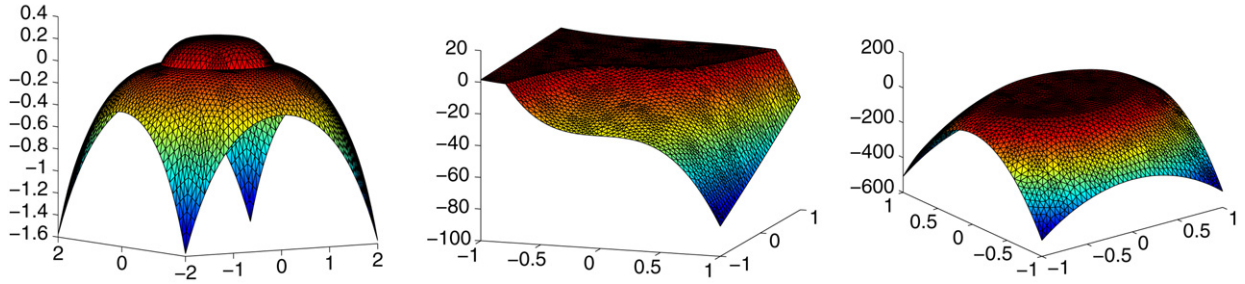


Fig. 3. From left to right: Exact solutions in Examples 5.1–5.3.

## 5. Numerical examples

In this section, we present several numerical examples to confirm our theoretical results. We test linear, subparametric, isoparametric and superparametric quadratic finite elements, which are denoted by  $P_1$  ( $m = 1$ ,  $p = 1$ ),  $P_2$  ( $m = 1$ ,  $p = 2$ ),  $isoP_2$  ( $m = 2$ ,  $p = 2$ ) and  $superP_2$  ( $m = 3$ ,  $p = 2$ ), respectively. In all our examples, we use interface-aligned triangulations, i.e., each element  $K$  of the triangulation satisfies either  $\bar{K} \cap \Gamma = \emptyset$ , or a single vertex of  $K$  lies on the interface  $\Gamma$  or all the nodal points of one edge (or one face) of  $K$  lie on  $\Gamma$ . Note that after each mesh refinement, some regularly refined elements near the interface have to be slightly adjusted to ensure that they are interface-aligned. Since the interfaces of the numerical examples are smooth, we have  $\delta = O(h^{m+1})$ .

**Example 5.1.** The computational domain  $\Omega$  is  $(-2, 2) \times (-2, 2)$ , and the interface  $\Gamma$  is the unit circle  $\{(x, y); x^2 + y^2 = 1\}$ . The exact solution  $u$  is set to be

$$u(x, y) = \begin{cases} \frac{1 - (x^2 + y^2)^2}{4\alpha_1}, & \text{if } x^2 + y^2 \leq 1; \\ \frac{1 - (x^2 + y^2)^2}{4\alpha_2}, & \text{if } x^2 + y^2 > 1, \end{cases}$$

which has vanishing jumps at the interface both in the solution and in the co-normal derivative. The exact solution is shown in the left picture of Fig. 3. Here we choose  $\alpha_1 = 1$ ,  $\alpha_2 = 10$ , and define the source function  $f$  to match the solution.

Fig. 4 shows the convergence behavior of the  $P_1$ ,  $P_2$ ,  $isoP_2$ , and  $superP_2$  elements. We note that the linear finite element solution gives the optimal first order convergence in the  $H^1$ -norm and second order convergence in the  $L^2$ -norm for  $\delta = O(h^2)$ . As the theory predicts, the affine-equivalent quadratic finite element solution can achieve only first order convergence in the  $H^1$ -norm and second order convergence in the  $L^2$ -norm due to the poor approximation of the interface ( $\delta = O(h^2)$ ); see Fig. 4(b). In other words, only a small gain in the accuracy is obtained by using  $P_2$  elements instead of linear  $P_1$  elements. Fig. 4(c) shows the convergence of  $isoP_2$  elements. In contrast to Theorem 4.12, we observe quadratic convergence order in the  $H^1$ -norm, which is better than the predicted  $O(h^{3/2})$ . However, this effect is explained by the symmetry properties of the circular interface. More precisely, a piecewise quadratic spline interpolating a circle gives  $\delta = O(h^4)$  and not only  $O(h^3)$ . For superparametric quadratic finite element, our numerical results are in agreement with our theory, see Fig. 4(d).

**Example 5.2.** The computational domain is  $(-1, 1) \times (-1, 1)$ , and the interface  $\Gamma$  is taken to be the cubic curve  $y = 2x^3$ . The exact solution  $u$  is given by

$$u(x, y) = \begin{cases} \frac{(y - 2x^3)^2 - 30(y - 2x^3)}{\alpha_1}, & \text{if } y \geq 2x^3; \\ \frac{(y - 2x^3)^2 - 30(y - 2x^3)}{\alpha_2}, & \text{if } y < 2x^3. \end{cases}$$

In our numerical test, we have chosen  $\alpha_1 = 20$ ,  $\alpha_2 = 1$ . The exact solution is shown in the middle picture of Fig. 3.

Fig. 5 shows the numerical results for this example. As in Example 5.1, the convergence behavior of the  $P_1$ ,  $P_2$  and  $superP_2$  elements confirm the theoretical prediction as shown in Figs. 5(a), 5(b), and 5(d). For the  $isoP_2$  case, one does not obtain the optimal convergence rate due to the poor interface approximation  $\delta = O(h^3)$ . In Fig. 5(c), the  $H^1$ -error appears to decay faster than the dashed reference line with slope 1.5. This is a preasymptotic phenomenon, since the global error consists of an  $O(h^{1.5})$  contribution from relatively few elements near the interface and an  $O(h^2)$  contribution from the elements away from the interface. Table 1 shows this effect in more detail, where the  $H^1$ -norms of the error  $e = u - u_h$  are listed for the mismatch region

$$S := (\Omega_{1,h} \setminus \Omega_1) \cup (\Omega_{2,h} \setminus \Omega_2) \quad (35)$$

and the region  $\Omega \setminus S$ . Table 1 also includes the number of degrees of freedom (Dofs), and the level of refinement (Level). Linear regression of the last three defects for the  $isoP_2$ -case shows a decay rate of 2.0007 for the  $H^1(\Omega \setminus S)$ -error and 1.5885 for the  $H^1(S)$ -error, which is in good agreement with Corollary 4.9 and Theorem 4.1.

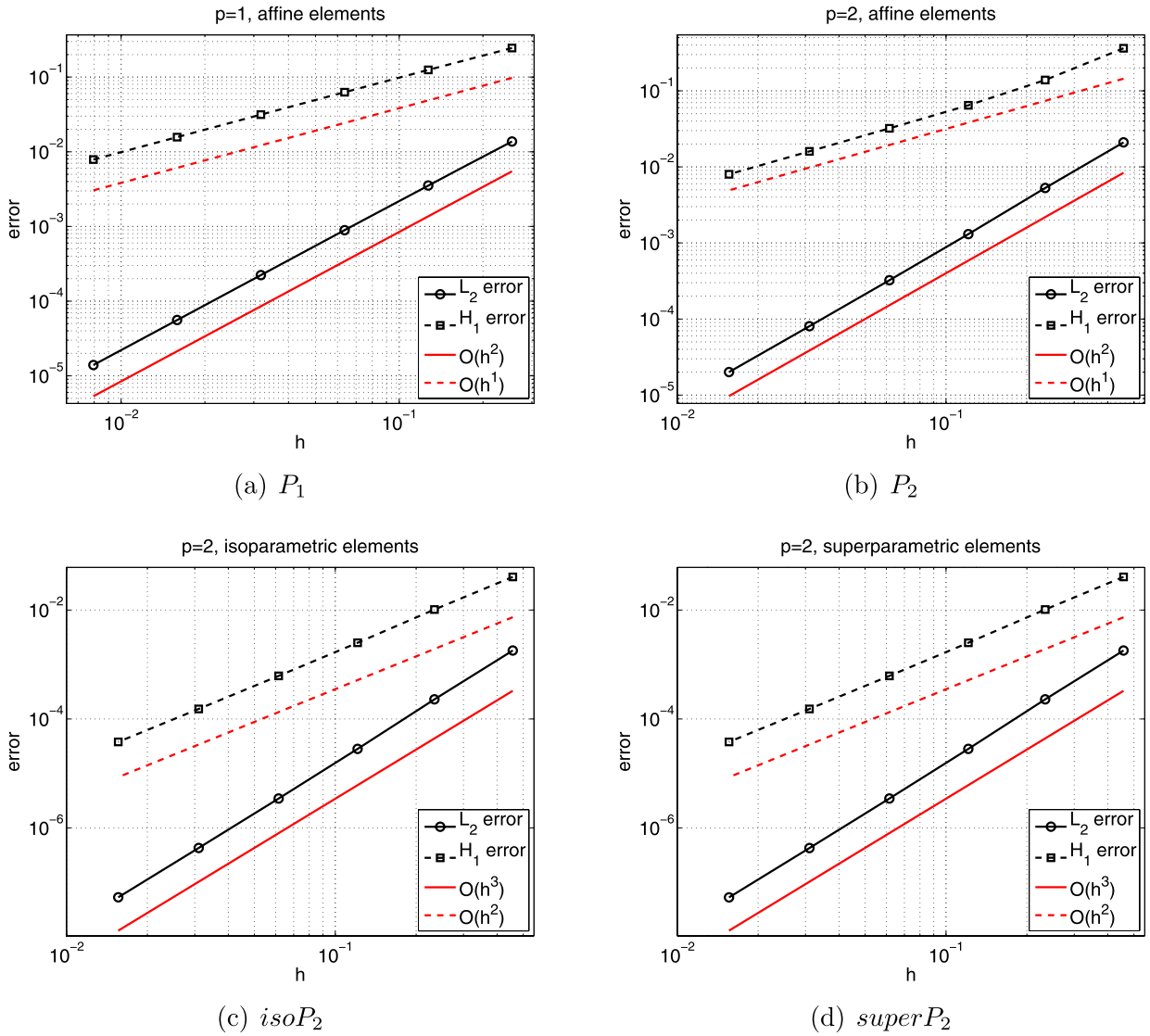


Fig. 4. Convergence of  $P_1$ ,  $P_2$ ,  $isoP_2$ , and  $superP_2$  elements in Example 5.1.

**Example 5.3.** The computational domain is  $(-1, 1) \times (-1, 1)$ , and the interface  $\Gamma$  is the ellipse given by  $\frac{16x^2}{9} + 4y^2 = 1$ . The exact solution  $u$  is chosen as

$$u(x, y) = \begin{cases} 10 - 10(x^2 + y^2)^2, & \text{if } \frac{16x^2}{9} + 4y^2 \leq 1; \\ 110 - 10(x^2 + y^2)^2 - \frac{1600}{9}x^2 - 400y^2, & \text{if } \frac{16x^2}{9} + 4y^2 > 1. \end{cases}$$

The solution  $u$  has non-vanishing interface values, and we choose piecewise smooth coefficients  $\alpha_1 = (-6220x^2 + 6561)/(180x^2 + 81)$ ,  $\alpha_2 = 1$  in the numerical test. The exact solution is shown in the right picture of Fig. 3.

The convergence results for  $P_1$ ,  $P_2$ ,  $isoP_2$  and  $superP_2$  elements are plotted in Figs. 6(a), 6(b), 6(c) and 6(d). Here, the suboptimal behavior of the  $isoP_2$  approximation (see Fig. 6(c)) can be observed from the beginning on.

For this example, we also study the convergence behavior away from the interface as analyzed in Theorem 4.8. In Fig. 7, we present the errors  $\|u - u_h\|_{H^1(S)}$  and  $\|u - u_h\|_{H^1(\Omega \setminus S)}$  for  $P_2$  and  $isoP_2$  elements, where the mismatch region  $S$  is given by (35). We note that the  $H^1(S)$ -error is very close to the  $H^1(\Omega)$ -error in Fig. 6. In fact, the  $H^1(\Omega \setminus S)$ -error is of higher order compared to  $H^1(S)$ . Applying Theorem 4.8 with  $\delta = O(h^2)$  for the case  $P_2$  and  $\delta = O(h^3)$  for the case  $isoP_2$  ( $s = 3$  in both cases), we obtain for the error  $\|u - u_h\|_{H^1(\Omega \setminus S)}$  the bounds  $O(h^{1.25})$  and  $O(h^2)$ , respectively. Numerically, we observe in Fig. 7 convergence  $O(h^{1.5061})$  and  $O(h^{2.0217})$ , respectively, by linear regression of the last three defects.

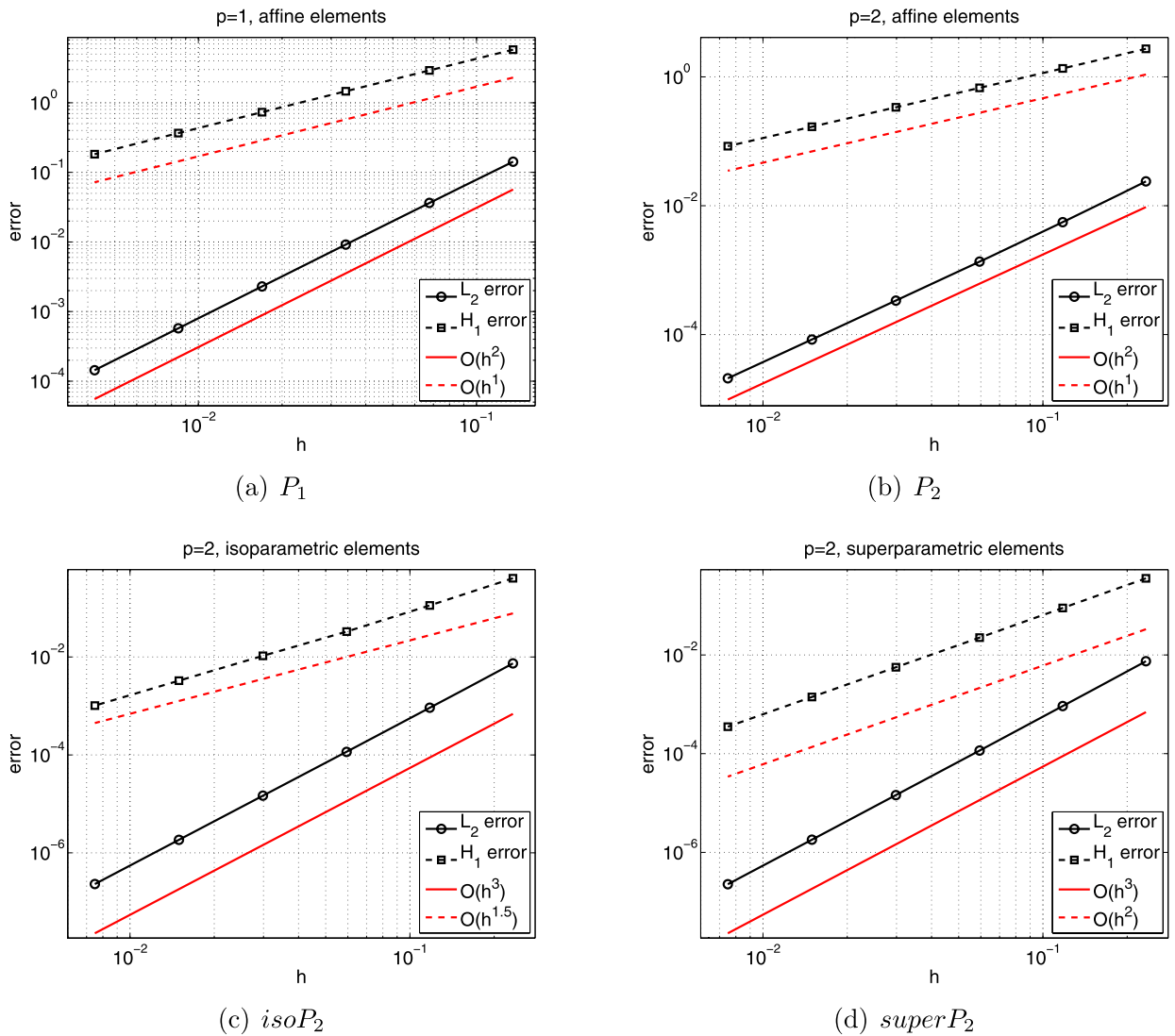


Fig. 5. Convergence of  $P_1$ ,  $P_2$ ,  $isoP_2$ ,  $superP_2$  elements in Example 5.2.

Table 1

$H^1$ -performance for  $P_2$  and  $isoP_2$  finite elements in Example 5.2.

Level	Dofs	h	$isoP_2$ element		$P_2$ element	
			$\ e\ _{H^1(\Omega \setminus S)}$	$\ e\ _{H^1(S)}$	$\ e\ _{H^1(\Omega \setminus S)}$	$\ e\ _{H^1(S)}$
1	751	2.3333(−1)	3.5494(−1)	1.9452(−1)	5.0444(−1)	2.6823(+0)
2	2,917	1.1771(−1)	8.9432(−2)	6.8844(−2)	1.5378(−1)	1.3448(+0)
3	11,497	5.9414(−2)	2.2461(−2)	2.4198(−2)	4.9227(−2)	6.7303(−1)
4	45,649	2.9848(−2)	6.4511(−3)	8.3592(−3)	1.6388(−2)	3.3662(−1)
5	181,921	1.4960(−2)	1.6391(−3)	2.8461(−3)	5.6011(−3)	1.6831(−1)
6	726,337	7.4888(−3)	4.0571(−4)	9.2957(−4)	1.9445(−3)	8.3974(−2)

**Example 5.4.** We consider the well-known benchmark test of a 2D elastic interface problem specified in Sukumar et al. [24]. The problem is radially symmetric with different material properties in concentric discs around the origin. The computational domain is  $\{(x, y); x^2 + y^2 < b^2\}$  with a circular interface  $\Gamma$  of the form  $x^2 + y^2 = a^2$ . The inner disc has Young's modulus  $E_1$  and Poisson ratio  $\nu_1$ , and the outer one  $E_2$  and  $\nu_2$ . At any point, the displacement vector can be written as  $\mathbf{u} = (u^r, u^\theta)$ , where  $u^r$  is the radial component, and  $u^\theta$  is the circumferential component of the displacement. The material



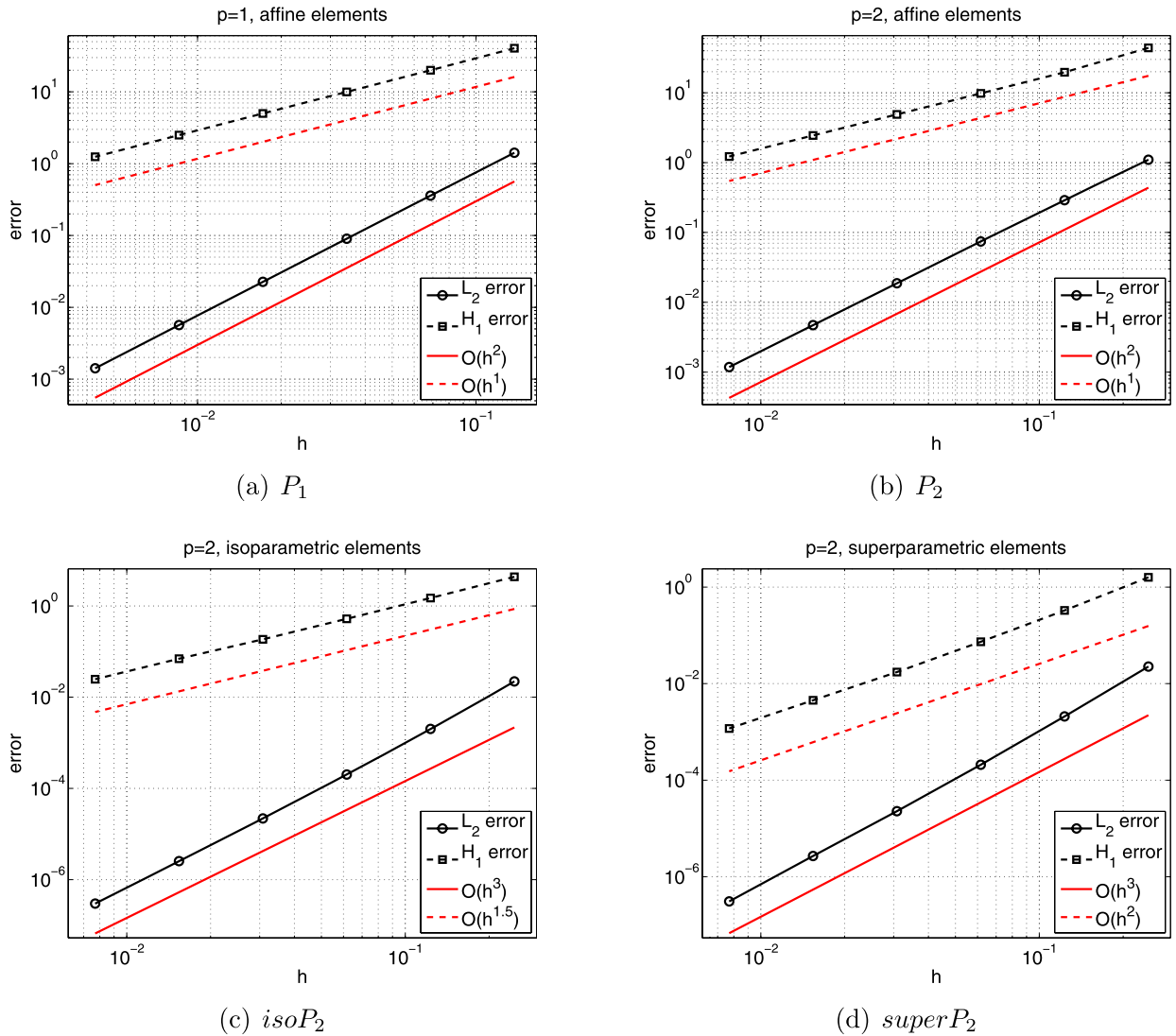


Fig. 6. Convergence of  $P_1$ ,  $P_2$ ,  $isoP_2$ ,  $superP_2$  elements for Example 5.3.

is subjected to the Dirichlet boundary condition  $\mathbf{u} = \mathbf{x}$  (in Cartesian coordinates), and the exact solution to the problem is given by

$$u^r(r) = \begin{cases} ((1 - \frac{b^2}{a^2})c + \frac{b^2}{a^2})r, & 0 \leq r \leq a; \\ (r - \frac{b^2}{r})c + \frac{b^2}{r}, & a \leq r \leq b, \end{cases}$$

with

$$c = \frac{(\lambda_1 + \mu_1 + \mu_2)b^2}{(\lambda_2 + \mu_2)a^2 + (\lambda_1 + \mu_1)(b^2 - a^2) + \mu_2 b^2}.$$

The Lamé constants  $\lambda_i$  and  $\mu_i$  are given by  $\lambda_i = \frac{E_i \nu_i}{(1+\nu_i)(1-2\nu_i)}$  and  $\mu_i = \frac{E_i}{2(1+\nu_i)}$ ,  $i = 1, 2$ . Following [24], we select  $E_1 = 1$ ,  $\nu_1 = 0.25$ ,  $E_2 = 10$ ,  $\nu_2 = 0.3$ ,  $a = 0.4$  and  $b = 2$ . The displacement of the exact solution as well as the errors in the  $H^1$ - and  $L^2$ -norm are shown in Fig. 8. As before, optimal convergence rates can be observed for linear finite elements.

**Example 5.5.** Our last example is a 3D interface problem. We take the cubic domain  $(-1, 1)^3$  as the computational domain with a spherical interface  $\Gamma: x^2 + y^2 + z^2 = 0.7^2$ . The exact solution  $u$  is given by

$$u(x, y) = \begin{cases} (0.7^2 - x^2 - y^2 - z^2)^2 / \alpha_1, & \text{if } x^2 + y^2 + z^2 \leq 0.7^2; \\ (0.7^2 - x^2 - y^2 - z^2)^2 / \alpha_2, & \text{if } x^2 + y^2 + z^2 > 0.7^2, \end{cases}$$

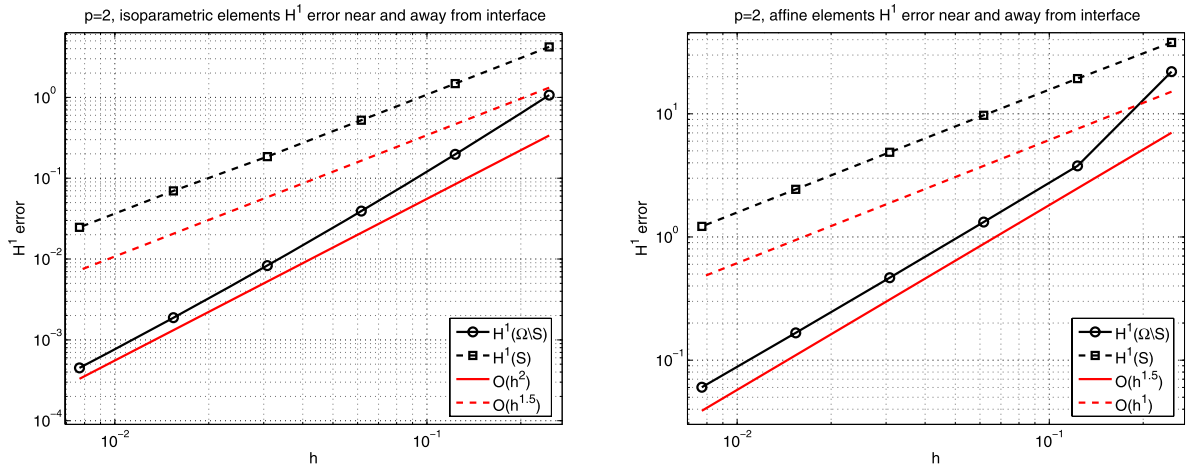


**Fig. 7.** Example 5.3: Convergence in  $H^1(\Omega \setminus S)$  and  $H^1(S)$  with  $S = (\Omega_{1,h} \setminus \Omega_1) \cup (\Omega_{2,h} \setminus \Omega_2)$ . Left: isoparametric elements,  $p = 2$ . Right: affine elements  $p = 2$ .

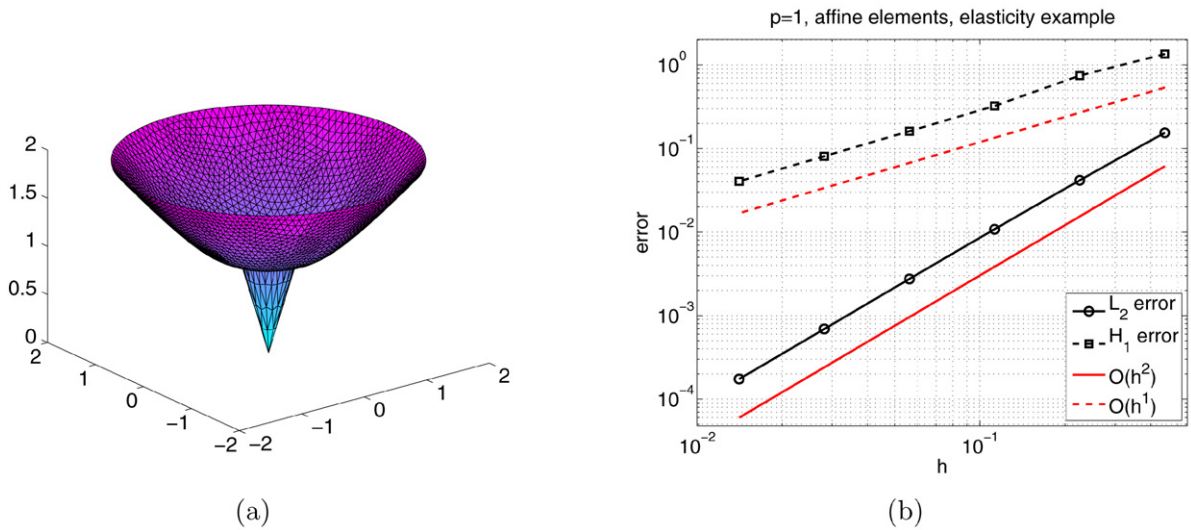


**Fig. 8.** (a) The exact solution in Example 5.4. (b) Convergence results for  $P_1$ .

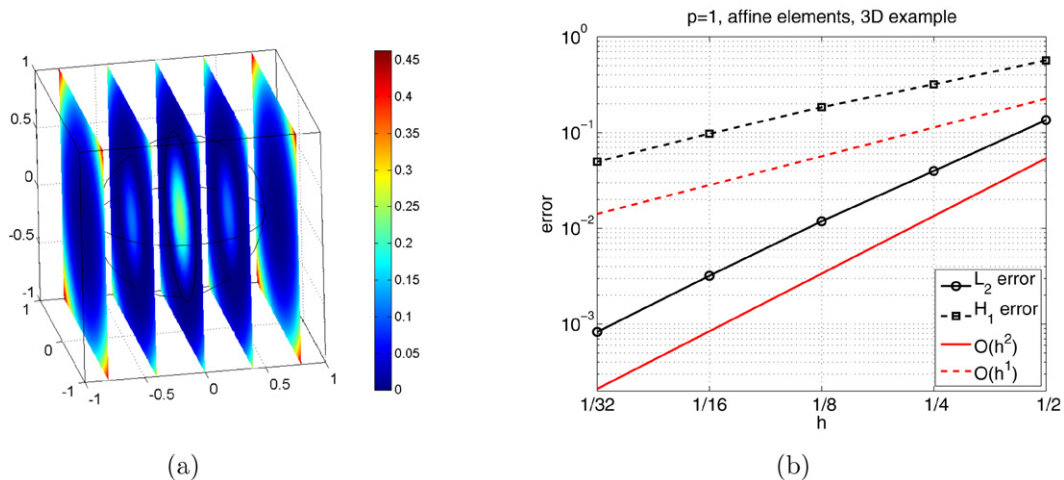


**Fig. 9.** (a) The exact solution in Example 5.5. (b) Convergence of  $P_1$  finite elements.

with the discontinuous coefficients chosen to be  $\alpha_1 = 1$  and  $\alpha_2 = 10$ , see Fig. 9. As in 2D, linear finite elements yield optimal convergence in both the  $L^2$ - and in the  $H^1$ -norm.

## References

- [1] R.A. Adams, Sobolev Spaces, Academic Press, New York/London, 1975.
- [2] I. Babuška, The finite element method for elliptic equations with discontinuous coefficients, *Computing* 5 (1970) 207–213.
- [3] J.W. Barrett, C.M. Elliott, Fitted and unfitted finite-element methods for elliptic equations with smooth interfaces, *IMA J. Numer. Anal.* 7 (1987) 283–300.
- [4] J.H. Bramble, J.T. King, A finite element method for interface problems in domains with smooth boundaries and interfaces, *Adv. Comput. Math.* 6 (1996) 109–138.
- [5] S.C. Brenner, L.R. Scott, *The Mathematical Theory of Finite Element Methods*, second ed., Springer-Verlag, 2002.
- [6] E. Burman, P. Hansbo, Interior penalty stabilized Lagrange multiplier methods for the finite element solution of elliptic interface problems, Preprint, Finite Element Center, 2007. *IMA Journal of Numerical Analysis*, in press, doi: 10.1093/imanum/drn081.
- [7] B. Camp, T. Lin, Y. Lin, W. Su, Quadratic immersed finite element spaces and their approximation capabilities, *Adv. Comput. Math.* 24 (2006) 81–112.
- [8] Z. Chen, J. Zou, Finite element methods and their convergence for elliptic and parabolic interface problems, *Numer. Math.* 79 (1998) 175–202.
- [9] P.G. Ciarlet, *The Finite Element Method for Elliptic Problems*, first ed., Studies in Mathematics and its Applications, North-Holland Pub. Co., Amsterdam/New York, 1978.
- [10] P. Clément, Approximation by finite element functions using local regularization, *RAIRO Anal. Numér.* 2 (1975) 77–84.
- [11] W.J. Gordon, Blending-function methods of bivariate and multivariate interpolation and approximation, *SIAM J. Numer. Anal.* 8 (1) (1971) 158–177.
- [12] W.J. Gordon, C.A. Hall, Construction of curvilinear coordinate systems and application to mesh generation, *Int. J. Numer. Meth. Eng.* 7 (1973) 461–477.
- [13] W.J. Gordon, C.A. Hall, Transfinite element methods: Blending-function interpolation over arbitrary curved element domains, *Numer. Math.* 21 (2) (1973) 109–129.
- [14] P. Grisvard, *Singularities in Boundary Value Problems*, Springer-Verlag/Masson, 1992.
- [15] A. Hansbo, P. Hansbo, An unfitted finite element method, based on Nitsche's method, for elliptic interface problems, *Comput. Meth. Appl. Mech. Eng.* 191 (47) (2002) 537–552.
- [16] J. Huang, J. Zou, A mortar element method for elliptic problems with discontinuous coefficients, *IMA J Numer. Anal.* 22 (2002) 549–576.
- [17] M. Lenoir, Optimal isoparametric finite elements and error estimates for domains involving curved boundaries, *SIAM J. Numer. Anal.* 23 (1986) 562–580.
- [18] Z. Li, K. Ito, *The Immersed Interface Method: Numerical Solutions of PDEs Involving Interfaces and Irregular Domains*, Society for Industrial and Applied Mathematics, Philadelphia, 2006.
- [19] Z. Li, T. Lin, X. Wu, New Cartesian grid methods for interface problem using finite element formulation, *Numer. Math.* 96 (2003) 61–98.
- [20] T. Lin, Y. Lin, W. Sun, Error estimation of a class of quadratic immersed finite element methods for elliptic interface problems, *Disc. Cont. Dynam. Sys. Series B* 7 (4) (2007) 807–823.
- [21] M. Plum, C. Wieners, Optimal a priori estimates for interface problems, *Numer. Math.* 95 (2003) 735–759.
- [22] L.R. Scott, Z. Zhang, Finite element interpolation of nonsmooth functions satisfying boundary conditions, *Math. Comp.* 54 (1990) 483–493.
- [23] E.M. Stein, *Singular Integrals and Differentiability Properties of Functions*, Princeton University Press, Princeton, 1970.
- [24] N. Sukumar, D.L. Chopp, N. Noës, T. Bleytschko, Modeling holes and inclusions by level sets in the extended finite-element method, *Comput. Meth. Appl. Mech. Eng.* 190 (2001) 6183–6200.
- [25] L. Tartar, *An Introduction to Sobolev Spaces and Interpolation Spaces*, Lecture Notes of the Unione Matematica Italiana, vol. 3, Springer, Berlin, 2007.
- [26] H. Triebel, *Interpolation Theory, Function Spaces, Differential Operators*, North-Holland, Amsterdam, 1978.
- [27] O.C. Zienkiewicz, R.L. Taylor, *The Finite Element Method*, vol. 1, The Basis, fifth ed., Butterworth-Heinemann, Oxford/Boston, 2000.